STRATEGIES FOR REMOVING BROMATE FROM DRINKING WATER

MOHAMED SIDDIQUI AND GARY AMY

PREPARED FOR:

CALIFORNIA URBAN WATER AGENCIES

WITH PARTICIPATION OF:

ALAMEDA COUNTY WATER DISTRICT
CONTRA COSTA WATER DISTRICT
LOS ANGELES DEPARTMENT OF WATER AND POWER
MWD OF SOUTHERN CALIFORNIA

UNIVERSITY OF COLORADO
AT BOULDER

JUNE 1995

Acknowledgments

Financial Help

This work has been supported by a consortium of California drinking water utilities; Metropolitan Water District of Southern California (MWD), Alameda County Water District (ACWD), Contra Costa Water District, and Los Angeles Department of Water & Power (LADWP) through the California Urban Water Agencies (CUWA), CA, with Lyle Hoag as the Project Manager. The authors also acknowledge the help of Stuart Krasner (MWDSC), Susan Teefy (ACWD), Gary Stolarik (LADWP), Larry McCollum and Ed Cummings (CCWD).

Graduate Student Researchers

The authors gratefully acknowledge the work of Wenyi Zhai, Kenan Ozekin and Paul Westerhoff, graduate students at the University of Colorado (CU), without whose help this project would have remained unfinished. The authors also thank Chandrakanth Mysore (CU) for measuring zeta potentials of different activated carbons.

Technical Help

The Authors also acknowledge the help of Lawrence DeMartino (Water Purification, Inc.), David McCarty and Karen Asher (Aquionics, Inc.) for their technical help and useful discussions.

Table of Contents

List of Tables

List of Figures

Bromate Removal By Activated Carbon

Bromate Removal By UV Irradiation

Executive Summary

As mandated by the 1986 Safe Drinking Water Act amendments, the USEPA is currently developing regulations for disinfection by-products (DBPs). In addition to potentially lowering the existing trihalomethanes (THMs) standard, the USEPA may regulate other DBPs. One ozone by-product under consideration is bromate.

The Surface Water Treatment Rule (SWTR) has established disinfection requirements for utilities based on specified disinfectant concentration and contact time (CT) values. Utilities must control pathogenic microorganisms while minimizing the formation of other harmful DBPs. Draft drinking water regulations in the U.S. will specify a maximum contaminant level (MCL) of 10 µg/L for bromate ion (BrO_3^-), an ozonation by-product produced during drinking water treatment.

To date, most BrO_3^- control strategies have involved inhibiting BrO_3^- formation through acid or ammonia addition. Adjustment to pH 6.0 prior to ozonation will significantly reduce BrO_3^- formation; however, acid addition may not be viable or cost effective for high alkalinity waters. Ammonia addition can theoretically tie up hypobromous acid/hypobromite ion ($HOBr/OBr^-$) as bromamine and scavenges free radicals thereby reducing the formation of BrO_3^-; however, the complexity of bromamine chemistry has yielded inconsistent BrO_3^- formation results ranging from reduction to no reduction in lab and pilot studies. Several different options to remove BrO_3^- after its formation, applicable to conventional surface water treatment plants contemplating the use of ozone at various points of application, have been evaluated: ferrous iron reduction (Fe^{2+}), activated carbon surface reduction (GAC), and ultraviolet irradiation (UV).

In all processes, chemical analysis of the treated water showed the formation of bromide ion (Br^-) indicating that chemical reduction of BrO_3^- is the significant mechanism; adsorption of BrO_3^- onto the surface of iron floc is insignificant. If Fe^{2+} is introduced following pre-ozonation, it can potentially function as both a BrO_3^- reducing agent and as a chemical coagulant to remove dissolved organic carbon (DOC), a measure of disinfection by-product (DBP) precursors. Surface reduction of BrO_3^- on either powdered or granular activated carbon has been observed, apparently preceded by an adsorption step. BrO_3^- removal is activated carbon specific, and not all carbons have shown the ability to reduce BrO_3^- to Br^-. Bromate destruction using a medium pressure lamp was much more effective than with a low pressure mercury lamp. Contact time as low as 5 seconds was sufficient to destroy bromate by more than 60% in a medium pressure arc lamp as opposed to a contact time of more than 10 minutes to achieve similar destruction using a low pressure lamp. pH had no significant effect whereas UV intensity had a positive effect on bromate destruction.

Part I
Scope and Background

This study of bromate removal after ozonation of drinking water was necessary because most natural water supplies contain trace levels of bromide ion (Br^-) and can form bromate levels in excess of the proposed maximum contaminant level (MCL) of bromate (10 µg/L). The D/DBP rule currently is scheduled for promulgation in December 1996 (Stage 1) with compliance requirements by surface water utilities serving more than 10,000 people in 1998. The stage 1 bromate MCL is to be proposed at 10 µg/L because of the inability of currently available analytical procedures to quantify lower levels in the field. EPA anticipates that by the time Stage 2 MCLs are promulgated (1999), analytical methodology will be improved and able to quantitate lower levels. Stage 1 D/DBP MCLs as proposed in April/May 1994 are as follows (agreed to by the Regulation Negotiation participants):

Total Trihalomethanes (TTHMS)	80 µg/L
Total Haloacetic Acids (THAAs)	60 µg/L
Bromate Ion	10 µg/L

Br^- occurs ubiquitously, with an average concentration in the U.S. of almost 100 µg/L (Amy et al, 1994). During the chemical oxidation and/or disinfection of natural waters containing Br^- with ozone, bromate ion (BrO_3^-) is formed at concentrations ranging from 0-50 µg/L under normal drinking water treatment conditions (Siddiqui and Amy, 1993, Krasner et al, 1993).

Ozone is a strong oxidant and it oxidizes bromide ion in water to bromate ion through two different pathways. BrO_3^- can form through both a molecular ozone (O_3) pathway and a hydroxyl radical ($OH\cdot$)* pathway, depending on the dissolved organic carbon (DOC), Br^- content, and pH of the source waters. By the molecular ozone pathway, Br^- is first oxidized by dissolved ozone to hypobromite ion (OBr^-) which is then further oxidized to BrO_3^- as shown below.

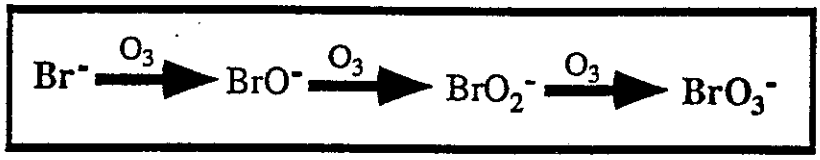

* OH radicals are produced as a result of the decomposition of molecular ozone at pH > 8. Molecular ozone (O_3) is highly selective as an oxidant whereas OH radicals are non-selective. The reaction rates of OH radicals with bromine species are many times faster than with molecular ozone.

This reaction is pH-dependent since OBr^- is in equilibrium with hypobromous acid (HOBr). The molecular ozone theory suggests that BrO_3^- formation is directly driven by dissolved ozone (DO_3) and the OH radical theory indicates that dissolved ozone plays only an indirect role by decomposing O_3 to produce radicals which further react with bromine species to produce BrO_3^- (Richardson et al., 1981 and Yates and Stenstrom, 1993) as shown below:

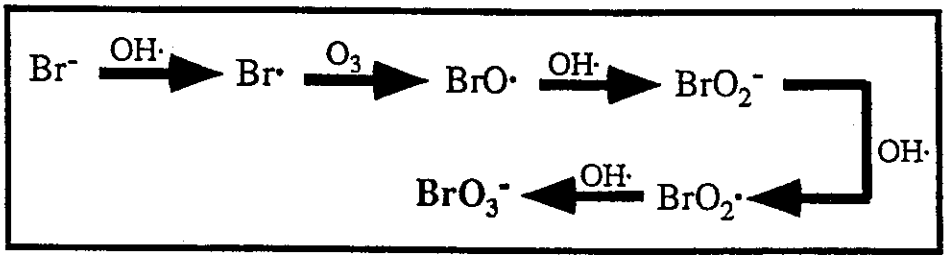

von Gunten and Hoigne (1993) have reported that 30-80% of BrO_3^- formation occurs through the molecular ozone pathway in contrast to Yates and Stenstrom (1993) who report less than 10% bromate formation through the molecular ozone pathway in natural source waters. This percentage may vary depending upon the background characteristics of the source water. Low DOC ground waters may produce bromate predominantly through a molecular ozone pathway whereas high DOC surface waters may produce bromate predominantly through a radical pathway.

Draft drinking water regulations in the U.S. will specify a maximum contaminant level (MCL) of 10 µg/L for BrO_3^- and a best available treatment (BAT) of pH adjustment (USEPA, 1994). To date, most BrO_3^- control strategies have involved inhibiting (minimizing) BrO_3^- formation through acid or ammonia addition (Gramith et al, 1993). Adjustment to pH 6.0 prior to ozonation will significantly reduce BrO_3^- formation; however, acid addition may not be viable or cost effective for high alkalinity waters. Ammonia addition can theoretically tie up $HOBr/OBr^-$ as bromamine and scavenges free radicals thereby reducing the formation of BrO_3^-; however, the complexity of bromamine chemistry has yielded inconsistent BrO_3^- formation results ranging from reduction to no reduction in lab and pilot studies (Krasner et al, 1993). Also, ammonia addition may result in a time-lag minimization of BrO_3^- formation due to secondary reactions between bromamines and ozone. The work reported herein involves removing BrO_3^- after its formation, when other control strategies are not cost effective and/or reliable. If the draft BrO_3^- MCL in the U.S. is lowered further, a combination of minimized production and subsequent removal may be required as a BrO_3^- control strategy.

While several researchers have performed detailed studies on BrO_3^- formation in ozonated water, there is a paucity of data relating to BrO_3^- removal from ozonated drinking waters. This work has evaluated several different options to remove BrO_3^- applicable to conventional surface treatment plants contemplating the use of ozone at various points of application. Several means of removing BrO_3^- after its formation have been evaluated: use of a chemical reducing agent/coagulant ($FeSO_4$), activated carbon, and ultraviolet irradiation.

Objectives

Tha main objectives of this research can be summarized as follows:

- determination of bromate formation potentials of various source waters.
- evaluation of bromate minimization using BAT of pH depression.
- evaluation of ferrous iron as a reductant to reduce bromate after pre-ozonation and to enhance coagulation.
- evaluation of activated carbon and ultraviolet irradiation for possible removal of bromate after intermediate ozonation.
- elucidation of removal mechanisms.

Part II
Experimental and Analytical Methods

Experimental Methods

Ferrous Iron [Fe(II)] Reduction Experiments. These experiments were performed using a conventional jar test apparatus. After adjusting samples to a desired pH, aliquots of sample were placed under a six-place stirrer. With the stirrer operating at 100 rpm, varying amounts of reductant/coagulant ($FeSO_4$. $7H_2O$) were added to the samples and the pH was allowed to drift from an initial pH to a final lower pH*. Each sample was flocculated for 30 minutes at 30 rpm after 1 minute of rapid mixing, settled for 1 hour, decanted, and filtered through a pre-washed 0.45 µm membrane filter (Millipore Corp., Type HC). These jar test experiments also permitted evaluation of Fe(II) coagulation for dissolved organic carbon (DOC) removal and monitoring of UV_{254} absorbance. The kinetics of BrO_3^- reduction were evaluated by collecting samples at different time intervals and immediately performing BrO_3^- analysis. The presence of residual Fe^{2+} did not interfere with measurements of BrO_3^-. Reagent grade ferrous sulfate ($FeSO_4$. $7H_2O$), ferric chloride ($FeCl_3$. $6H_2O$), and alum ($Al_2(SO_4)_3$. $18H_2O$) were used (Aldrich Chemical Company, Milwaukee, WI). Suwannee river humic material was used to evaluate the effect of DOC on BrO_3^- reduction (International Humic Society, Golden, CO).

Powdered Activated Carbon (PAC) Experiments. BrO_3^- reduction experiments using powdered activated carbon (PAC) (<325 mesh) were performed by the batch shaker test. The appropriate PAC dose (mg/L) was introduced into 100 mL amber bottles. The bottles were placed on a shaker table for a specified time (15 min - 24 hrs) and filtered through pre-washed 0.45 µm filters (Millipore Corp., Type HC). A complete list of activated carbons used along with their total surface area is given in Table 2.1.

Table 2.1. List of Different Activated Carbons Used

Carbon	Type	Manufacturer	Total Surface Area, m^2/g
D-10	PAC	American Norit Co, GA	575
CX0655	PAC	MCB Chemicals, OH	N/A
WPH	PAC	Calgon Carbon, PA	650
BL	PAC	Calgon Carbon, PA	1000
HDB	PAC	American Norit Co, GA	600
F-400	GAC	Calgon Carbon, PA	900
F-300	GAC	Calgon Carbon, PA	1100
PK	GAC	American Norit Co, GA	590

* For kinetic experiments pH was held constant by adding NaOH

Activated Carbon (GAC-RSSCT) Experiments. Rapid small-scale column testing (RSSCT) experiments were performed to evaluate bromate removal by granular activated carbon (GAC) under dynamic, continuous-flow conditions (Figure 2.1). Typical operating conditions for RSSCT evaluation are given in Table 2.2. Design parameters and scale-up have been addressed through similitude relationship between RSSCTs and pilot-scale plants. Although this scale-up is based on removal of DOC, this approach can still provide a preliminary assessment of the feasibility of GAC for BrO_3^- reduction.

Table 2.2. Rapid Small-Scale Column Testing (RSSCT) Operating Conditions

Design Parameters	RSSCT	Pilot-Scale*
Bulk Density, g/mL**	0.5	0.5
Particle Radius, mm	0.1	0.5
Mesh Size	50 x 80	12 x 40
EBCT, min	0.32	8-10
Flow Rate, mL/min	12-30	170
Column Diameter, cm	1.1	5.0
Time of Operation, days	2-5	50-100
Water Volume Required, L	120	12258
Glass Column Length, cm	14	80
Mass of Carbon, g	7	—

Ultraviolet Irradiation Equipment. Ultraviolet experiments were conducted in four different types of apparatus fitted with different UV lamps surrounded by different quartz tubing (Table 2.3).

Table 2.3. Summary of UV Apparatuses Used

Parameter	Units	Ultradynamics[1] (Low Pressure) A	Aquafine[2] (Low Pressure) B	Anatel[3] (Low Pressure) C	Aquionics[4] (Medium Pressure) D
Lamp Length	cm	30	30	5	25
Lamp Output	Watts	50	17	8-24	3500
Lamp Intensity	$\mu W/cm^2$	6,000	2,100	900-2,500	$5x10^5$
Flow Rate	gpm	2	1	100 mL/min	50
Reactor Vol	mL	500	100	15	1850
Quartz Type	--	Q1	Q2	Q3	Q4
Wavelength, λ	nm	99% 254	95% 250-260 5% 180-200	90% 250-260 10% 180-200	100% 200-300
Contact Time	min	2-15	2-15	30-120 sec	4-30 sec

[1] Ultradynamics Corpration, CA
[2] Aquafine, Valencia, CA
[3] Anatel, Boulder, CO
[4] Aquionmics, Erlanger, KY

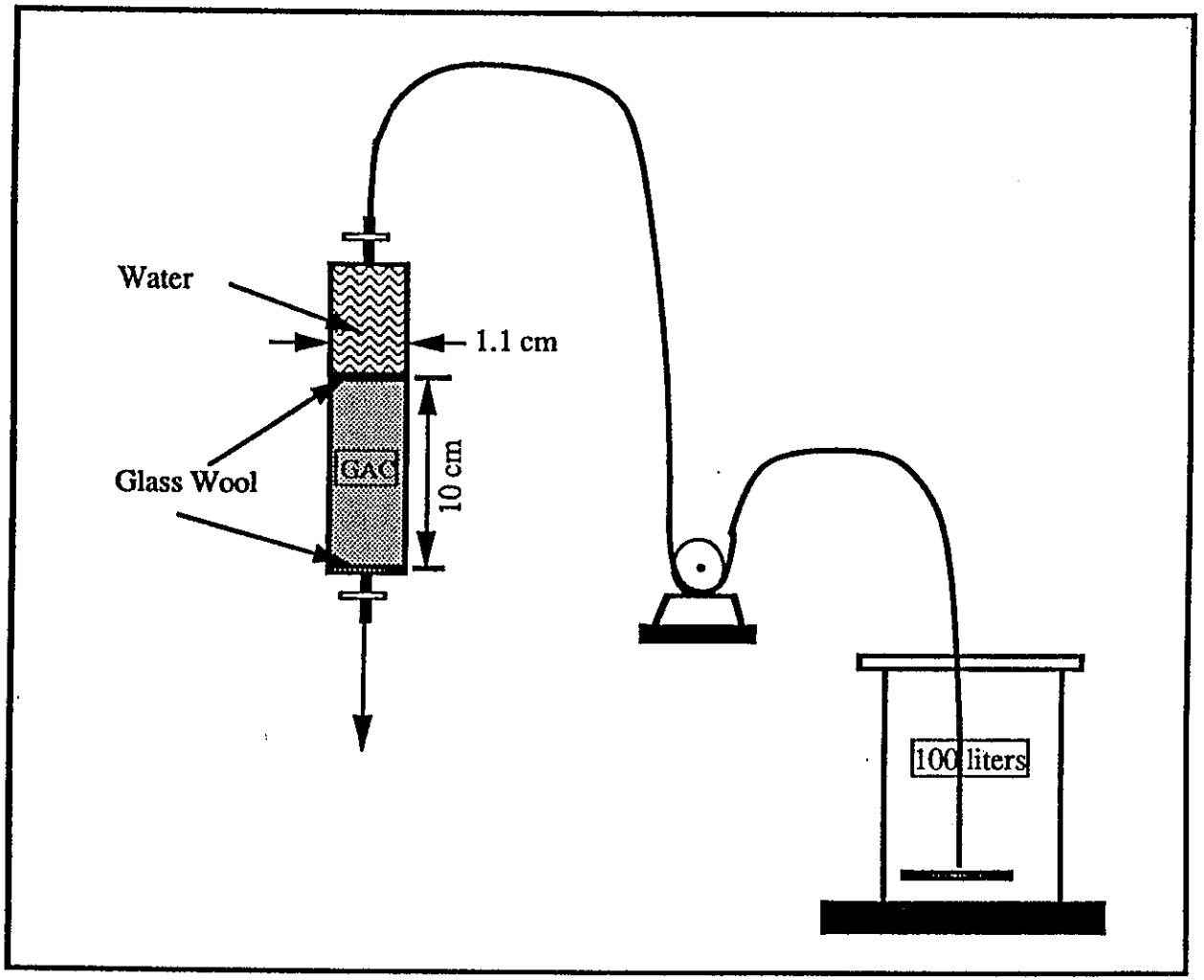

Figure 2.1 RSSCT Experimental Set Up

Relevant spectrophotometric and thermodynamic properties of bromate and other bromate decomposition products are given in Table 2.4. It is evident from this table that bromate absorbs predominantly at 190-200 range wavelength.

Table 2.4. Properties of Bromate, Bromite, and Hypobromite ions in Aqueous Solution

Ion	λmax nm	ΔH_f^o kcal mol^{-1}	ΔG_f^o kcal mol^{-1}	Oxidation product
BrO_3^-	195	- 15.95	+ 4.55	BrO_4^-
BrO_2^-	260	- 9.9	+ 2.1	BrO_3^-
BrO^-	330	–	–	BrO_2^-

ΔH_f^o = heat of formation; ΔG_f^o = free energy change

UV Batch Experiments were performed using the traditional UV apparatus (Instruments A and B; Figures 2.2 and 2.3) normally employed for disinfection, with most radiations emitted at 254 nm. Solutions of BrO_3^- were prepared in DOC-free water (MQW) and different source waters, and irradiated at different contact times ranging from 5-25 minutes in a cylindrical reactor (B) and an annular reactor (A) equipped with a low pressure mercury lamp.

UV Continuous Flow Experiments were evaluated in a 15 ml reactor (Instrument C), with an initial BrO_3^- concentration in a higher range than might be encountered in water treatment (50-100 µg/L). Solutions of BrO_3^- were prepared in MQW and source waters, and irradiated in a cylindrical reactor equipped with a variable intensity low pressure mercury lamp. The intensity of the UV lamp was varied by varying the current through the lamp, and the irradiance of the UV lamp (180-254 nm) was measured with a UV intensity meter (850-2000 µW/cm^2). Experiments were performed for contact times ranging from 10 sec to 100 sec.

A low pressure mercury vapor lamp has traditionally been used for UV disinfection. With an input power of 15-80 watts, the UV frequency emitted is ≈254 nm in the germicidal range and 185 nm in the shorter wave length range. UV intensity can be varied by increasing the number of lamps, changing voltage, or by employing a **medium pressure lamp.** Emitting a high output in the 200-300 nm range, a single medium pressure tube can replace up to 50 low pressure arc-tubes. In addition, the medium pressure lamps are unaffected by fluid temperature. Continuous flow experiments were performed using a medium pressure lamp (I=500 m W/cm^2) for contact times ranging from 5 sec to 15 sec (instrument D).

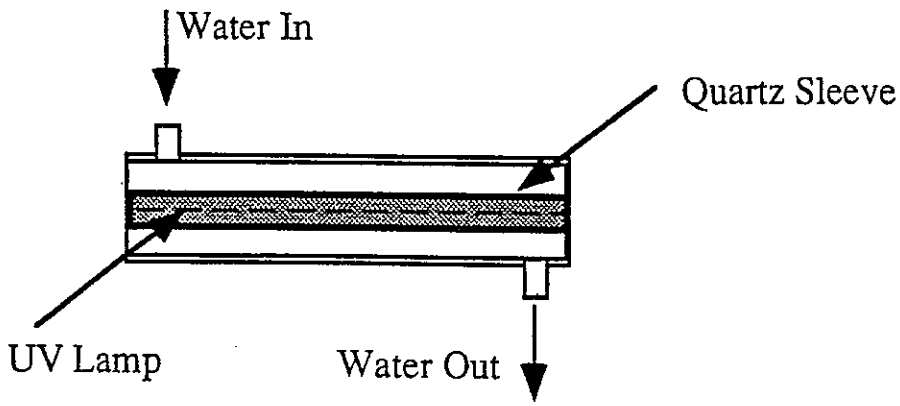

Figure 2.2. Ultradynamics Annular Reactor (A)

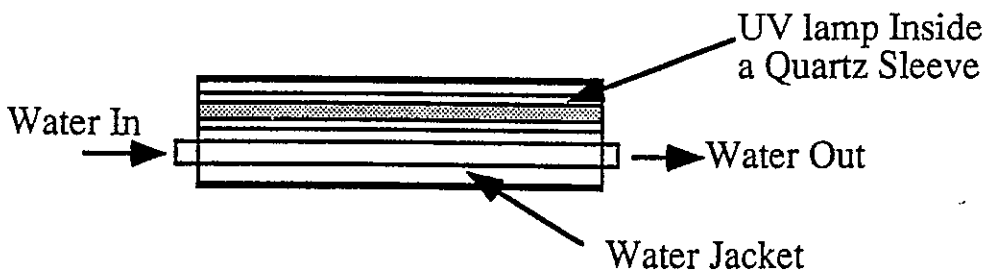

Figure 2.3. Aquafine Low Pressure Reactor (B)

Ozonation. True batch bench scale ozonation system was employed to study bromate formation potentials. The ozone generation system consists of an OREC O3V5-O (Ozone Research & Equipment Corporation) 0.25 lb/day generator and a 0.5 liter capacity glass reactor (washing bottle). Ozone stock solution (35-40 mg/L) was generated from pure oxygen with ozone and carrier gas admitted to the reactor in a semi-batch mode. True Batch experiments were conducted by diluting a raw water with a concentrated ozone stock solution to achieve a final initial ozone concentration (3 to 5 mg/L). Dilution of the raw water constituents must be considered. In contrast to semi-batch ozonation where ozone is applied over a period of time (5 to 15 minutes) and reactions can occur during ozone application, true batch experiments introduces 100% of the aqueous ozone to the system at time zero.

Analytical Methods

Br^- and BrO_3^- measurements were accomplished by ion chromatography (IC) using a Dionex 4500i series system (Dionex Corp., Sunnyvale, CA) with an IonPac AS9-SC column and an anion micromembrane suppresssor column (AMMS-II) (a revised version of USEPA method 300.0). A 2 mM Na_2CO_3/0.75 mM $NaHCO_3$ eluent was used for Br^- measurement and a 40 mM H_3BO_3/20 mM NaOH eluent was employed for BrO_3^- determination. Minimum detection limit (MDL) for BrO_3^- using borate eluent was 2-5 µg/L. For samples with high chloride ion (Cl^-) content, a syringe silver cartridge filter (silver coating on high capacity strong acid cation exchanger) was used to precipitate Cl^- as silver chloride prior to IC analysis to minimize its interference with BrO_3^- measurement. Conductivity detector response was almost perfectly linear ($R^2 \geq 0.99$) for standards ranging from 10 to 100 µg Br^-/L and from 2 to 50 µg BrO_3^-/L.

Dissolved organic carbon (DOC) was measured using a Shimadzu-5000 TOC analyzer fitted with an autosampler (Shimadzu Scientific Insts., Columbia, MD). Samples were filtered through a pre-washed 0.45 µm nylon membrane filter in order to minimize interferences caused by particulate matter. For the source waters evaluated, DOC levels were within 5% of (total) TOC levels.

UV absorbance measurements at 254 nm were made using a Shimadzu-160 UV/VIS spectrophotometer. Special experiments were conducted to investigate the effect of dissolved iron on the UV_{254} absorbance of natural waters and the results showed that higher Fe(II) concentrations result in significant increases in the UV_{254} absorbance of the water, representing a positive interference.

Ferrous iron (Fe^{2+}) concentration was measured (spectrophotometrically) with T.P.T.Z (2,4,6-tri-pyridyl-triazine) with a detection limit of 0.01 mg Fe^{2+}/L (Dougan and Wilson, 1983).

Dissolved Oxygen (DO). These measurements were made using a DO meter fitted with an oxygen selective membrane (YSI MODEL).

Inorganic composition (titanium, vanadium, strontium, iron, and other metals) of activated carbons was measured by inductively coupled plasma emission spectroscopy (ICP) with a detection limit of 5 µg/L (Aro Corp., MI). Sulfur was measured by first converting sulfur to sulfur dioxide at 850 ^{o}C and measuring sulfur dioxide by using infrared detection. Concentration of metals on the surface of the carbons was measured by a x-ray fluorescence spectrophotometer (Kevex Corp., CA).

Isoelectric points of different carbons were evaluated by measuring zeta potential at various pH levels with a Zeta Plus instrument equipped with a laser doppler velocimetry unit (Brookhaven Instrument Corporation, NY).

Residual Ozone. Ozone residual were measured using Method 4500-O3 A as described in Standards Methods, ,17th Edition (1989).

Routine water quality parameters such as pH, alkalinity, hardness, and sulfate were measured according to Standard Methods (APHA, 1989).

A summary of analytical methods along with their minimum reporting levels (MRL) are summarized in Table 2.5. Precision, reported in terms of percentage coefficient of variation (% C.V) is also shown in Table 2.5.

Table 2.5. Summary of Analytical Methods and Detection Limits

Parameter	Symbol	Units	Method	MRL	% C.V
Bromide	Br^-	µg/L	EPA-300	10	0.85
Bromate	BrO_3^-	µg/L	EPA-300	2-5	0.91
Dissolved Ozone	O_3	mg/L	4500-O3	0.05	0.25
Fe (II)	Fe^{2+}	mg/L	Colorometric	0.1	1.12
Bromine	$HOBr/OBr^-$	µg/L	Colorometric	0.05	1.24
Dissolved Oxygen	O_2	mg/L	O_2 selective Probe	0.2	0.88

Part III

Bromate Formation Potential Upon Ozonation

Source Water Characteristics

Surface waters evaluated included State Project Water, CA (SPW), Colorado River Water, CA (CRW), Contra Costa Water, CA (CCW), Alameda County water, CA (ACW), Los Angeles Aqueduct water, CA (LAW), Silver Lake Water, CO (SLW), and DOC-free (≤ 0.2 mg/L) Milli-Q water (MQW). A sample of SPW and CCW was taken from the Sacramento-San Joaquin river delta, which is subject to saltwater intrusion. SLW is a sub-alpine reservoir in the Rocky mountains. CRW bromide levels may be influenced by salt deposits (connate sea water) on the western slope of Colorado. Important characteristics of the source waters studied are summarized in Table 3.1.

Samples of chemically-pretreated water (coagulated and settled) were also obtained for some activated carbon and UV irradiation experiments.

Table 3.1. Source Water Characteristics

Source	Date	UVA per cm	DOC mg/L	pH	Alk mg/L	Br^- ug/L
SPW-I	10/08/93	0.107	4.4	8.0	82	155
SPW-II	03/22/94	0.097	3.6	8.0	90	145
SPW-II*	03/22/94	0.031	1.8	7.8	70	145
CCW-I	12/05/93	0.065	3.0	7.9	87	155
CCW-II	05/10/94	0.115	3.8	8.0	90	145
CCW-II*	05/10/94	0.033	1.7	6.8	80	145
LAW	01/05/94	0.097	5.1	7.9	--	35
LAW*	01/05/94	0.033	2.4	7.8	--	35
CRW	11/10/93	0.045	3.4	8.2	120	70
SLW	09/07/93	0.065	2.3	7.0	18	<10
ACW	12/23/93	0.085	3.4	7.6	64	175
ACW*	12/23/93	0.028	2.2	6.8	50	175
KCY	05/05/94	--	1.5	7.2	--	--

* Coagulated source waters

Experimental Matrix. The experimental matrix and ranges of variables studied for bromate formation potential in different source waters is shown in Table 3.2.

Table 3.2. Experimental Matrix for Bromate Formation Potential* Experiments

Source	Br^- = Ambient			Br^- = 250 µg/L			Br^- = 500 µg/L		
	6.0	7.0	8.0	6.0	7.0	8.0	6.0	7.0	8.0
CRW	√	√	√	√	√	√	√	√	√
SPW	√	√	√	√	√	√	√	√	√
CCW	√	√	√	√	√	√	√	√	√
ACW	√	√	√	√	√	√	√	√	√
LAW	√	√	√	√	√	√	√	√	√
SLW	√	√	√	√	√	√	√	√	√
MQW	√	√	√	√	√	√	√	√	√

For all these experiments three different ozone doses [0.5, 1.0, 1.5 $mgO_3/mgDOC$] were employed

Effect of Water Quality Variables on Bromate Formation

To investigate bromate formation potentials, a series of laboratory-scale studies were carried out in which various source waters were treated with various doses of ozone in the presence of different amounts of Br^- and at varying pH levels and the results are summarized below.

1. Effect of pH: The effect of pH on bromate formation at three different pH levels of 6.0, 7.0, and 8.0 was evaluated. Generally, bromate formation increased on increasing the pH from 6.0 to 8.0. CRW showed the highest bromate potential, with bromide being equal. This can be attributed to the lower ozone demand in CRW because of lower MW DOC it contains which is more resistant to coagulation. Naturally occurring organic material varies widely in different source waters and does not react similarly upon oxidation by ozone. LAW showed the least bromate formation potential, ostensibly due to its higher DOC. The results are summarized in Tables 3.3-3.7. These tables indicate that bromate formation was favored at higher pH (up to 8.0) because of an equilibrium favoring OBr^- and higher efficiency of OH radical production. pH levels beyond 9.0 accelerates the decomposition of ozone to oxygen and water rather than OH radicals thereby reducing the formation of bromate. The threshold ozone concentrations were found to be dependent on pH levels as shown in Table 3.8 (see also Figures 3.1 and 3.2). Average threshold ozone concentration at ambient pH levels was found to be O_3/DOC=0.5 mg/mg indicating that (except LAW) all source waters examined have the potential to form bromate in excess of the proposed MCL of 10 μg/L.

Table 3.8. Threshold Ozone Doses at Ambient Br^-* Levels

Source Water Ozonated	pH=6		pH=7		pH=8	
	$\frac{O_3}{DOC}$	O_3 mg/L	$\frac{O_3}{DOC}$	O_3 mg/L	$\frac{O_3}{DOC}$	O_3 mg/L
CRW	1.5	5.1	0.8	2.7	0.5	1.7
SPW-I	1.0	4.4	0.6	2.6	0.5	2.2
ACW-I	0.7	2.4	0.6	2.0	0.4	1.4
CCW-I	1.0	3.0	0.7	2.1	0.6	1.8

2. Effect of Ozone Dose. Ozone dosage plays a critical role in the formation of bromate. Many constituents in water including organic matter present an ozone demand. If ozone is added to meet this demand, bromate can be produced when

* ozone threshold concentration is that concentration below which no bromate formation occurs and it is determined by following the formation of bromate at various ozone doses at a fixed bromide level and other conditions.

Table 3.3. Bromate Formation Potentials for CRW

Ozone Dose (O_3/DOC)	Bromide µg/L	BrO_3^- µg/L		
		6.0	7.0	8.0
0.5	70	BDL*	BDL	6
1.0	70	BDL	12	16
1.5	70	8	21	30
0.5	250	BDL	11	12
1.0	250	14	30	42
1.5	250	35	47	70
0.5	500	BDL	14	19
1.0	500	33	70	75
1.5	500	66	160	176

*BDL = below detection limit

Table 3.4. Bromate Formation Potentials for SPW

Ozone Dose (O_3/DOC)	Bromide µg/L	BrO_3^- µg/L		
		6.0	7.0	8.0
0.5	155	BDL	4	6
1.0	155	6	13	18
1.5	155	12	32	42
0.5	250	BDL	8	13
1.0	250	8	24	29
1.5	250	16	41	49
0.5	500	3	13	19
1.0	500	11	35	45
1.5	500	22	51	66

Table 3.5. Bromate Formation Potentials for CCW

Ozone Dose (O_3/DOC)	Bromide µg/L	BrO_3^- µg/L		
		6.0	7.0	8.0
0.5	155	BDL	BDL	BDL
1.0	155	9	14	15
1.5	155	18	29	30
0.5	250	BDL	BDL	BDL
1.0	250	14	15	19
1.5	250	31	32	45
0.5	500	BDL	BDL	BDL
1.0	500	16	40	61
1.5	500	31	86	99

Table 3.6. Bromate Formation Potentials for ACW

Ozone Dose (O_3/DOC)	Bromide µg/L	BrO_3^- µg/L		
		6.0	7.0	8.0
0.5	175	6	12	16
1.0	175	12	29	38
1.5	175	24	36	49
0.5	250	7	14	22
1.0	250	13	29	41
1.5	250	25	41	60
0.5	500	7	19	26
1.0	500	26	40	49
1.5	500	52	95	112

Table 3.7. Bromate Formation in LAW

Ozone Dose (O_3/DOC)	Bromide µg/L	BrO_3^- µg/L		
		6.0	7.0	8.0
0.5	35	BDL	BDL	BDL
1.0	35	BDL	BDL	BDL
1.5	35	BDL	BDL	BDL
0.5	250	BDL	BDL	BDL
1.0	250	BDL	BDL	BDL
1.5	250	4	31	52
0.5	500	BDL	BDL	BDL
1.0	500	BDL	36	47
1.5	500	BDL	75	98

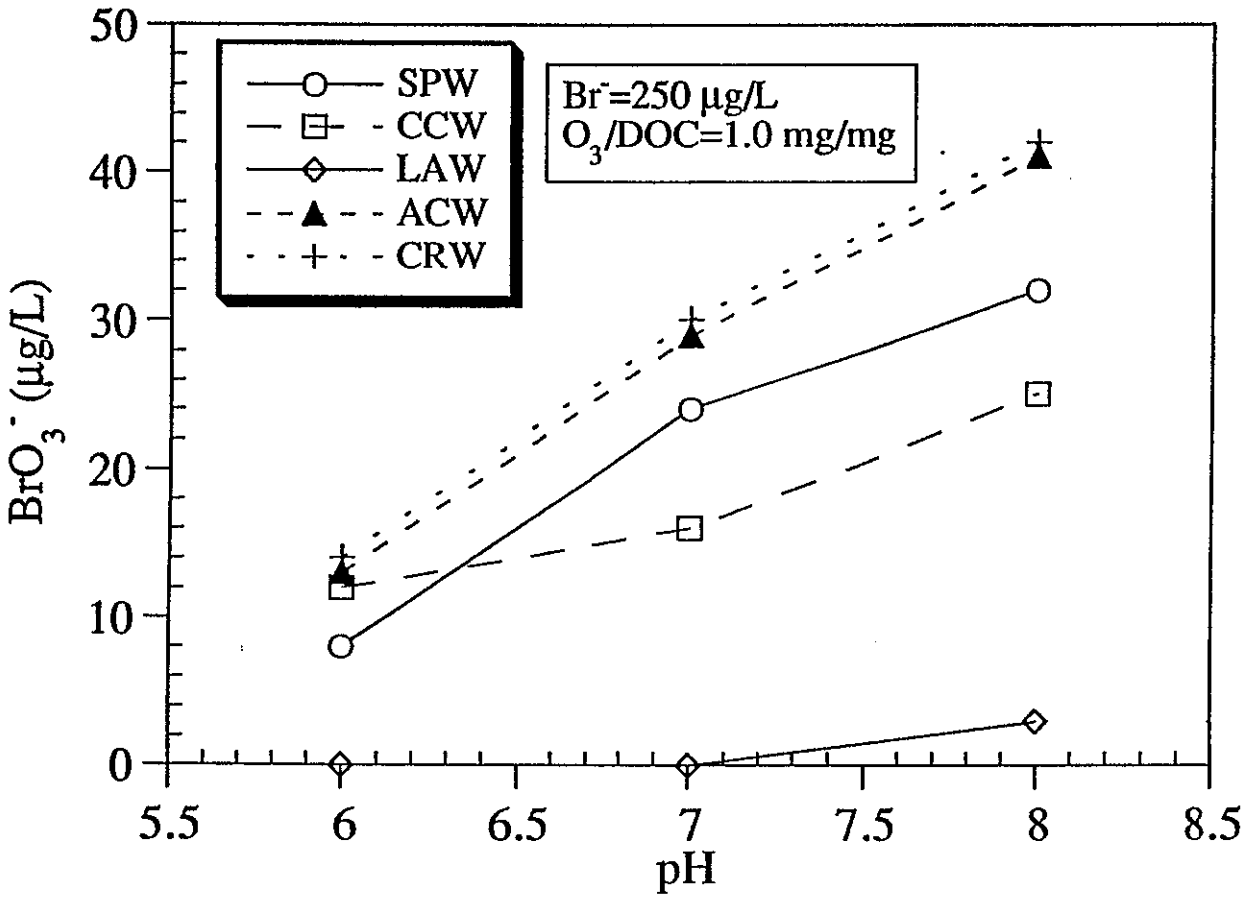

Figure 3.1. Effect of pH on BrO_3^- Formation

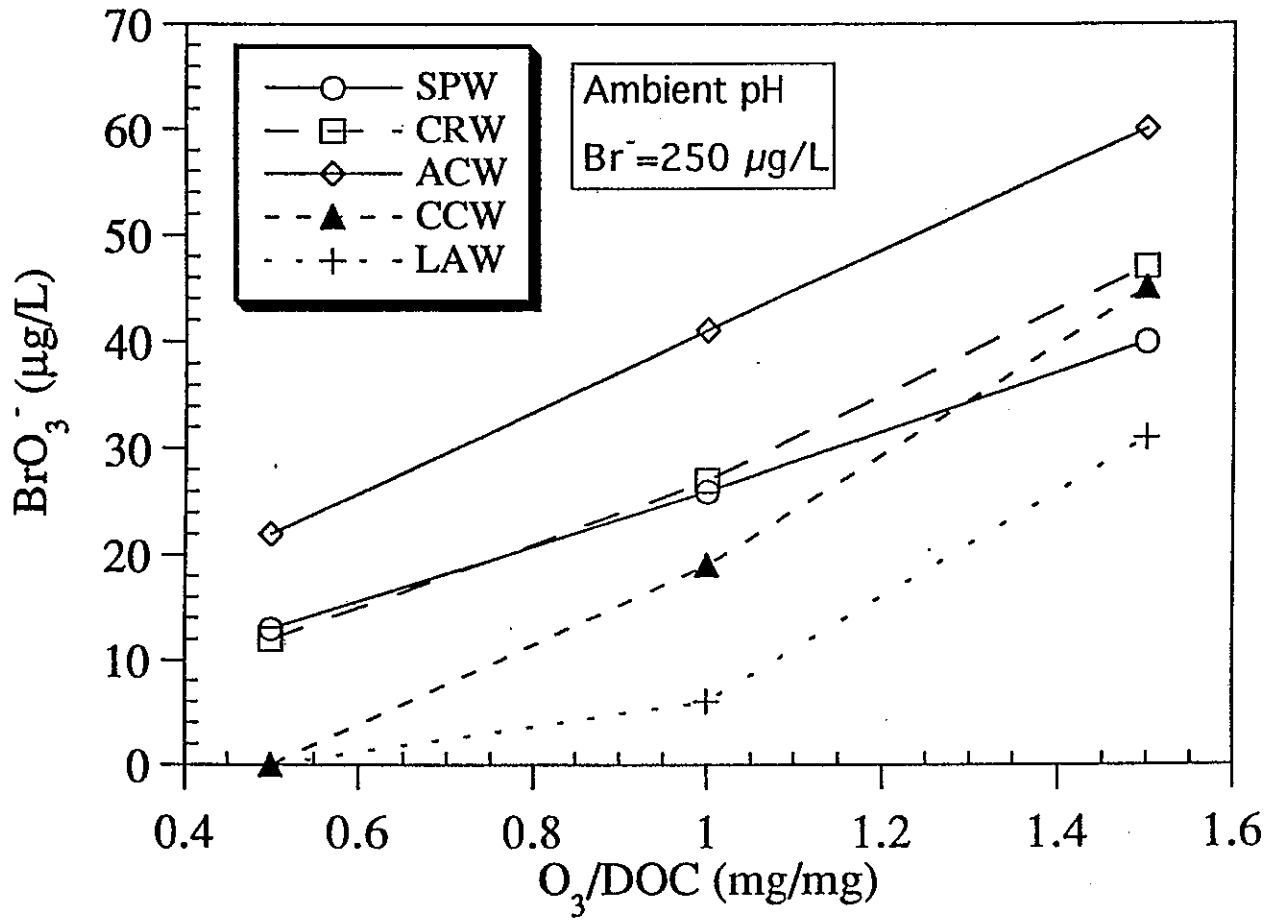

Figure 3.2. Effect of Ozone Dose on BrO_3^- Formation

sufficient bromide is present. The effect of ozone dose on bromate formation was evaluated at three different ozone doses: 0.5, 1, and 1.5 mg ozone/mg DOC. Higher bromate formation was observed at higher ozone doses. The doses shown in Tables 3.3-3.7 are transferred ozone doses. Threshold ozone doses at different pH levels and bromide concentrations are shown in Tables 3.8 and 3.9. Ozone concentrations as low as 1 mg/L can potentially produce bromate in excess of 10 µg/L. LAW water was found to possess a relatively higher ozone threshold concentration due to higher ozone demand.

Table 3.9. Threshold Ozone Doses at Various Br^- Levels

Source Water Ozonated	Br=amb.		Br=250 µg/L		Br=500 µg/L	
	$\frac{O_3}{DOC}$	O_3 mg/L	$\frac{O_3}{DOC}$	O_3 mg/L	$\frac{O_3}{DOC}$	O_3 mg/L
CRW	0.5	1.7	0.4	1.4	0.3	1.0
SPW-I	0.5	2.2	0.3	1.3	0.3	1.3
LAW	>1.5	--	1.2	5.4	0.7	3.2
ACW-I	0.4	1.4	0.25	0.8	<0.25	<0.8
CCW-I	0.6	1.8	0.75	2.2	0.55	1.6

3. Effect of Bromide Ion Concentration. The effect of bromide ion concentration on bromate formation was evaluated at ambient bromide level, 250, and 500 µg/L. The data show that as Br^- increased, with dissolved organic matter and ozone dosage remaining the same, the formation of bromate increased for each source water. The threshold bromide levels for different source waters are shown in Table 3.10.

For two of six source waters (SLW, LAW), the ambient bromide level was less than 40 µg/L, hence bromate was not detected at ambient Br^- concentrations. For four of six source waters (CRW, SPW, CCW, ACW) tested, ambient Br level was 80-180 µg/L and bromate was detected at levels of 6-49 µg/L for ozone doses ranging from 1.2-4.5 mg/L.

Table 3.10. Threshold Br^- Concentration at ambient pH Levels

Source Water	$\frac{O_3}{DOC} = 0.5 \frac{mg}{mg}$	$\frac{O_3}{DOC} = 0.5 \frac{mg}{mg}$	$\frac{O_3}{DOC} = 0.5 \frac{mg}{mg}$
CRW	70	<70	<70
SPW	155	<155	<155
LAW	500	320	250
ACW	<175	<175	<175
CCW	400	155	<155

4. Effect of Source Water Characteristics. Colorado river water was found to possess the highest bromate formation potential and LAW water exhibited the least bromate formation potential because of low and high DOC concentrations respectively. Naturally occurring organic material varies widely in different source waters and does not react similarly upon oxidation by ozone. Higher molecular weight DOC can exert a higher ozone demand than lower molecular weight DOC. The DOC of CRW is comprised of more lower molecular weight material as opposed to more higher molecular weight material in the other sources.

5. Effect of Alkalinity. Alkalinity has been shown to stabilize dissolved ozone in water thereby increasing its half life. Also alkalinity has been shown to enhance the formation of bromate through carbonate radicals. This can be explained by the enhanced bromate formation in CRW, which found to contain highest amount of alkalinity. Our research has shown that contribution towards bromate ion formation due to carbonate radicals at pH=8.5 is much more predominant than at pH=6.5 (30% vs 5%). This is presumably due to a shift towards HCO_3^- ions from CO_3^{2-} ions ($HCO_3^- <==> CO_3^{2-} + H^+$; pK_a=10.3) and higher production of OH radicals. CO_3^{2-} ions reacts about 12 times faster with OH radicals than HCO_3^- ions and therefore have a larger scavenging effect. The mechanism of bromate formation through carbonate radicals is shown below.

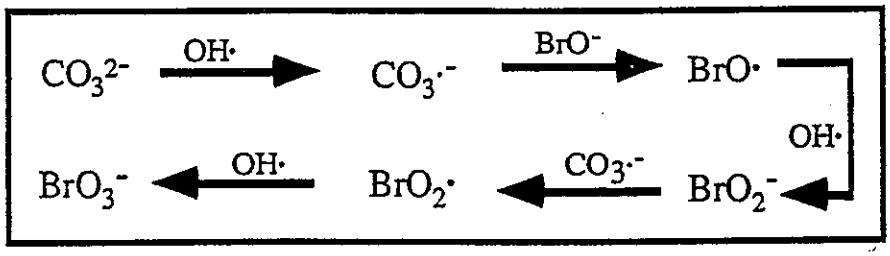

Most source waters examined in this research had ambient pH levels around 8.0 and a significant amount of alkalinity is present as CO_3^{2-}. The ratio of alkalinity normalized to DOC was found to follow the order, for different source waters, as follows:

$$[Alk/DOC]_{CRW} > [Alk/DOC]_{SPW} > [Alk/DOC]_{CCW} > [Alk/DOC]_{ACW} > [Alk/DOC]_{LAW} > [Alk/DOC]_{SLW}$$

Conclusions

With the exception of LAW, all source waters produced bromate higher than the anticipated MCL of 10 ug/L under ambient conditions. Lowering pH levels from 8.0 to 6.0 reduced bromate formation by more than 50%. The threshold ozone concentration is strongly dependent upon the pH and bromide content of source waters.

Part IV

Bromate Reduction By Ferrous Sulfate (After Pre-Ozonation)

Introduction. Bromate formed during pre-ozonation of drinking water can potentially be removed during the coagulation step of the process train by switching from normal coagulants to a ferrous salt. The potential points of bromate removal after pre-ozonation are shown in Figure 4.1.

Experimental Matrix. The experimental matrix and ranges of variables studied for bromate reduction using ferrous sulfate in different source waters is shown in Table 4.1.

Kinetics of Bromate Reduction. Chemical reduction of BrO_3^- to Br^- is feasible through the use of ferrous iron (Fe^{2+}) as a reducing agent which itself is then converted to ferric iron (Fe^{3+}). Also, in an ozonated water, there will be ample dissolved oxygen (DO) to convert any remaining Fe(II) to Fe(III). The resultant $Fe(OH)_3$ can function as a coagulant. Relevant reactions are summarized below:

$$BrO_3^- + 6Fe^{2+} + 6H^+ \Longrightarrow Br^- + 6Fe^{3+} + 3H_2O \quad \text{----[4.1]}$$

$$4Fe^{2+} + O_2 + 4H^+ \Longrightarrow 4Fe^{3+} + 2H_2O \quad \text{----[4.2]}$$

$$Fe^{3+} + 3HCO_3^- \Longrightarrow Fe(OH)_{3(s)} + 3CO_2 \quad \text{----[4.3]}$$

From equation [4.1], the rate law for bromate reduction by Fe^{2+} is given by the following equation [found to be first order with respect to both BrO_3^- and Fe^{2+}]:

$$\frac{d[BrO_3^-]}{dt} = -k[BrO_3^-][Fe^{2+}][H^+] \quad \text{----[4.4]}$$

and since $[Fe^{2+}]$ is present in excess when compared to $[BrO_3^-]$, the rate expression at a constant pH can be written as:

$$\frac{d[BrO_3^-]}{dt} = -k'[BrO_3^-] \quad \text{----[4.5]}$$

where $k'=k[Fe^{2+}][10^{-pH}]$ is the pseudo first order rate constant which is dependent on initial Fe^{2+} concentration and pH.

Table 4.1. Experimental Matrix for Bromate Reduction By Ferrous Sulfate*

Source	BrO_3^- = 15 µg/L**			BrO_3^- = 25 µg/L**			BrO_3^- = 50 µg/L**			BrO_3^- = 75 µg/L**		
	6.5	7.5	8.5	6.5	7.5	8.5	6.5	7.5	8.5	6.5	7.5	8.5
CRW	√	√	√	√	√	√	√	√	√	√	√	√
SPW	√	√	√	√	√	√	√	√	√	√	√	√
CCW	√	√	√	√	√	√	√	√	√	√	√	√
ACW	—	—	—	√	√	√	√	√	√	√	√	√
LAW	—	—	—	√	√	√	√	√	√	√	√	√
SLW	—	—	—	√	√	√	√	√	√	√	√	√
MQW	—	—	—	√	√	√	√	√	√	√	√	√

* all of these experiments were performed at four different $FeSO_4$. $7H_2O$ doses [25, 50, 75, 100 mg/L]

** these are spiked levels and that waters were not ozonated prior to Fe(II) addition

Bromate removal by common coagulants. Several commonly used coagulant chemicals have been investigated to quantify the extent of adsorption of the BrO_3^- to the surface of the precipitate phase, or its reduction to Br^- by Fe^{2+} (Figure 4.2). Trivalent metal hydroxides, such as $Al(OH)_3(s)$ and $Fe(OH)_3(s)$, exhibit a pH-dependent amphoteric behavior. At a pH below the pH_{zpc} (isolectric point), the floc surface will be positive, a condition favorable for the adsorption of BrO_3^-. Alum (Al^{3+}=60 mg/L) removed up to 5% BrO_3^- as opposed to up to 20% removal by ferric chloride (Fe^{3+}=60 mg/L); both presumably due to adsorption of BrO_3^- to the Al(OH)3 (pH_{zpc}=7.0) or $Fe(OH)_3$ (pH_{zpc}=8.5) floc surface. These experiments illustrate the poor capabilities of coagulating agents and the apparent inability of metal hydroxide adsorption to significantly reduce BrO_3^- concentrations in natural waters.

Effect of Treatment and Water Quality Parameters

1. Effect of Fe^{2+} Dose. Fe^{2+} doses ranging from 5- 25 mg/L were evaluated at different pH levels and with initial bromate levels ranging from 15-75 ug/L (Figures 4.3, 4.4 and 4.5). A ferrous salt concentration of 50 mg/L is sufficient to reduce the bromate concentration from 25 ug/L to less than the proposed MCL of 10 ug/L in most source waters at ambient pH levels. The effect of iron dose was more dramatic at lower pH levels. Approximately 60-80% of the initial bromide in bromate was recovered, confirming chemical reduction.

2. Effect of pH. The effect of pH on BrO_3^- reduction by Fe^{2+} was evaluated over the range of 6.5 to 8.5 in different source waters (Figures 4.3 and 4.5). Equation (1) would predict better BrO_3^- reduction at lower pH, a trend observed in the experiments. Upon Fe^{2+} addition, the pH of MQW and SLW dropped to approximately 5.5 from an initial pH of 7.5, while the final pH levels of CRW and SPW dropped by less than one pH unit because of less buffering capacity in SLW. Also Figure 4.6 shows the effect of pH on the value for the first order rate constant for the reduction of BrO_3^- in MQW (pH=6.5, 8.0; Fe^{2+}=20 mg/L). Also the disappearance of Fe^{2+} was slower at lower pH levels due higher stability of Fe^{2+} (equation 4.2; Figure 4.7).

3. Effect of Source Water. Better BrO_3^- removal was observed in CRW than in SPW, and Fe^{2+} persisted somewhat longer in CRW. SPW is more amenable to DOC removal by coagulation whereas CRW is more resistant and hence better iron complexation with the NOM in SPW is expected. Figure 4.8 shows the first order plots of BrO_3^- removal for CRW and SPW (pH=8.0, Fe^{2+}=15 mg/L, BrO_3^- = 50 µg/L). Psuedo first order rate constants (k', min^{-1}) evaluated using rate

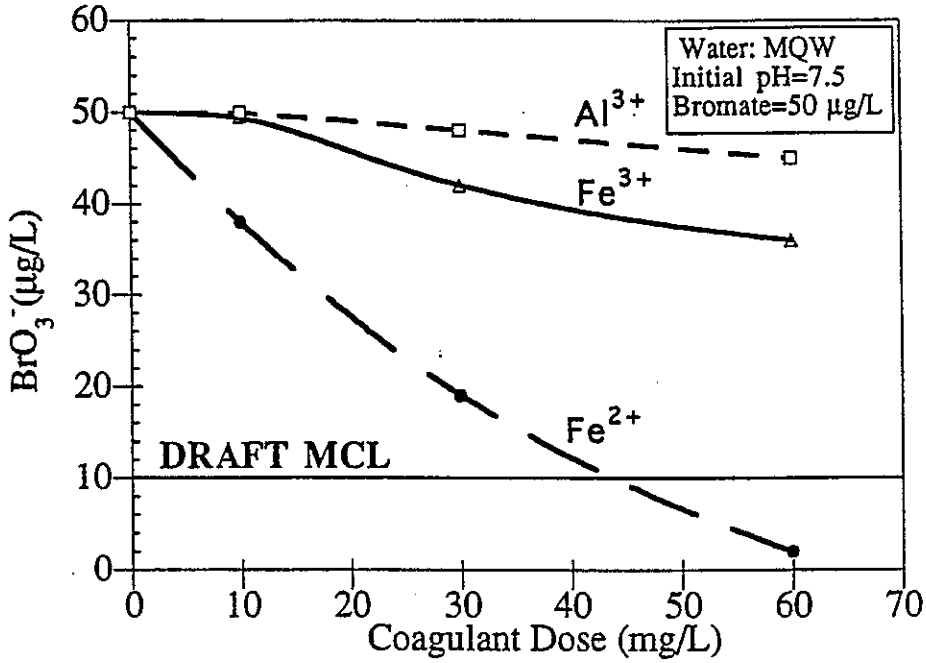

Figure 4.2. Bromate Reduction With Common Coagulants

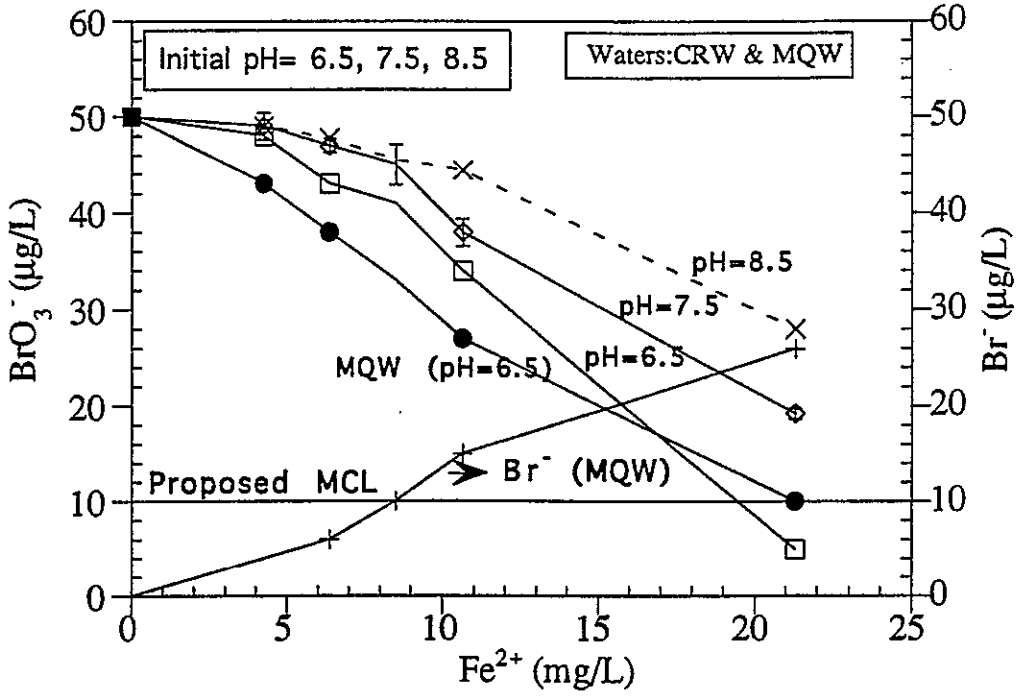

Figure 4.3. Effect of Fe^{2+} and pH on BrO_3^- Reduction and Bromide Formation

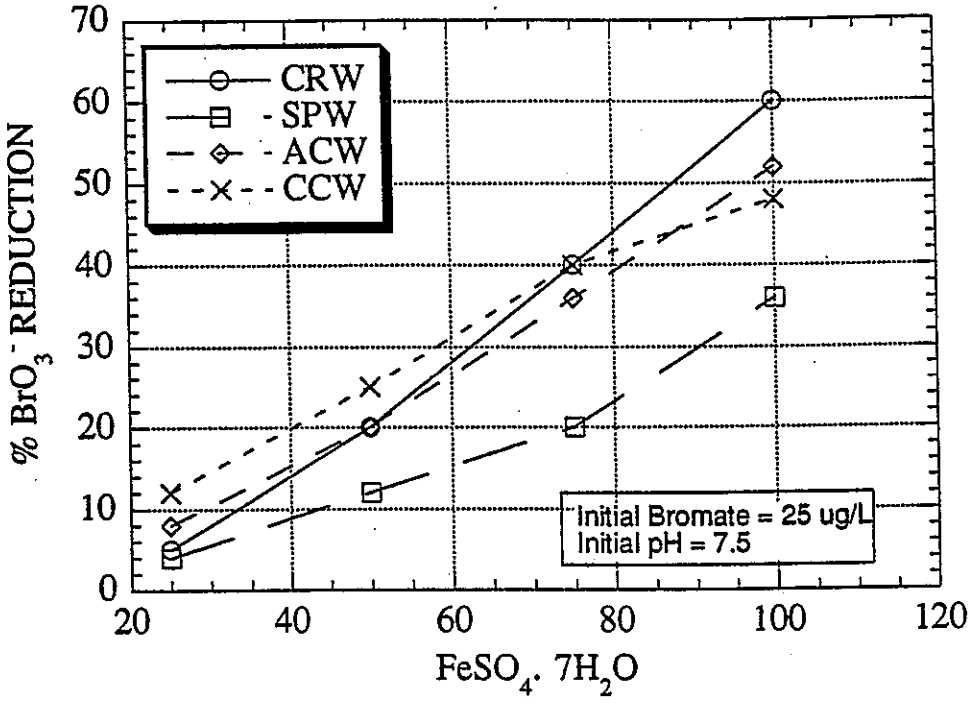

Figure 4.4. % Bromate Reduction vs Source Waters

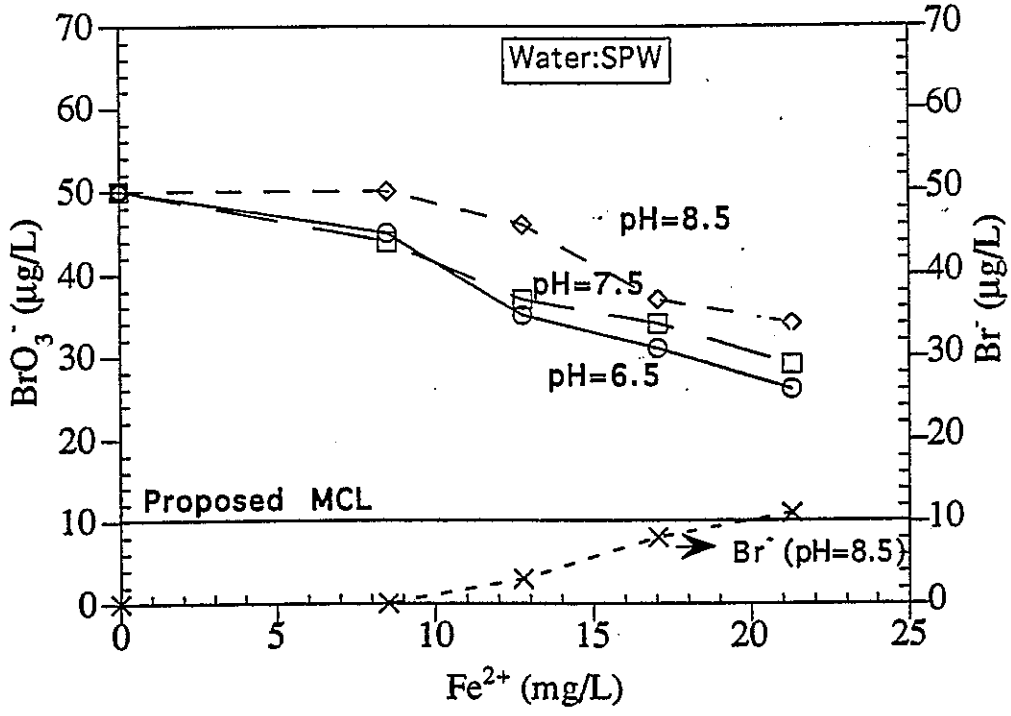

Figure 4.5. Effect of Fe^{2+} and pH on BrO_3^- Reduction and Bromide Formation

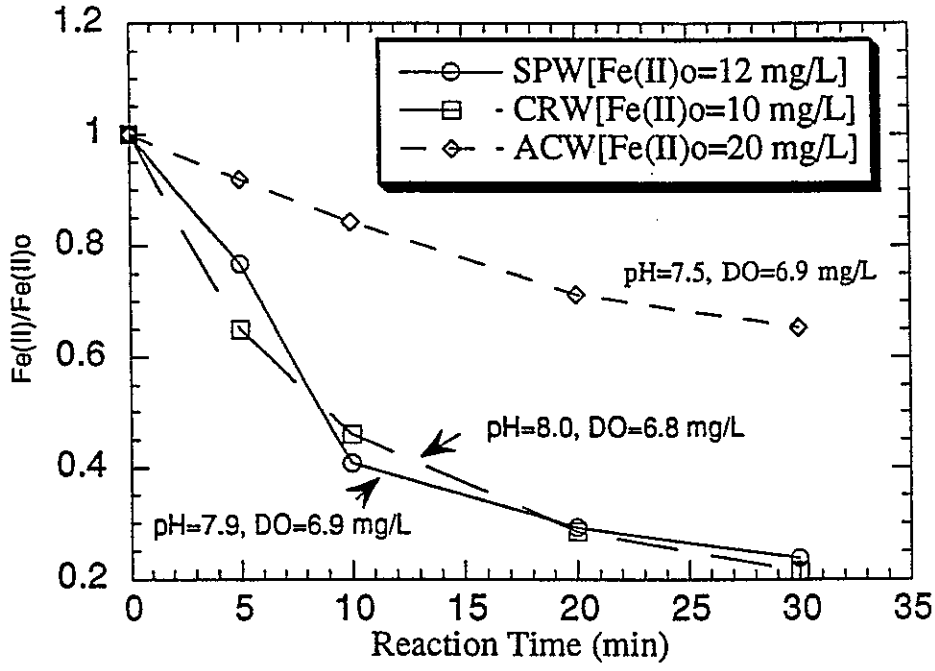

Figure 4.6. Kinetics of Fe(II) Disappearance in Source Waters

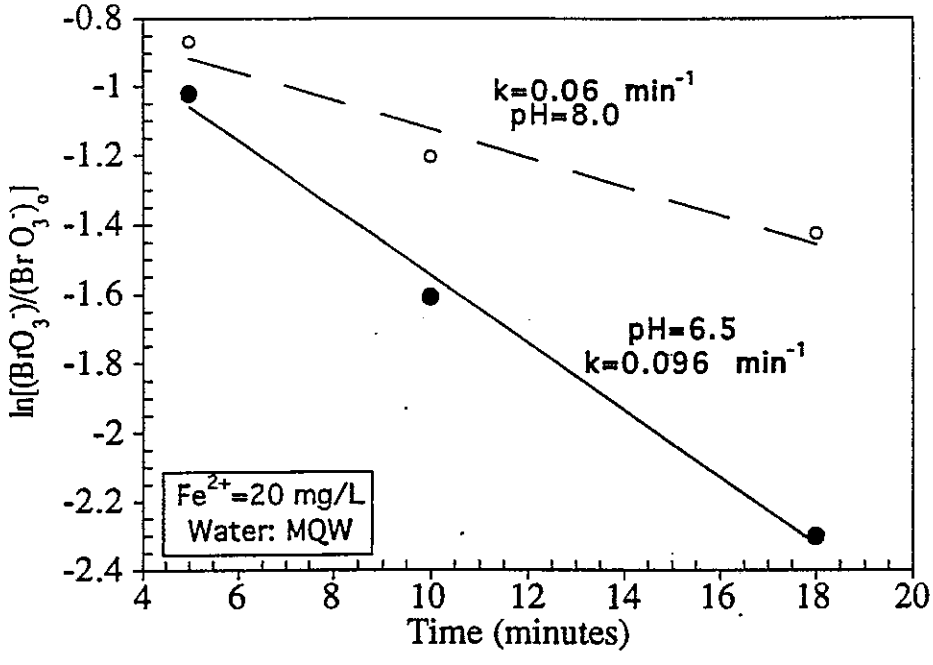

Figure 4.7. Effect of pH on the Rate of Reduction of BrO_3^-

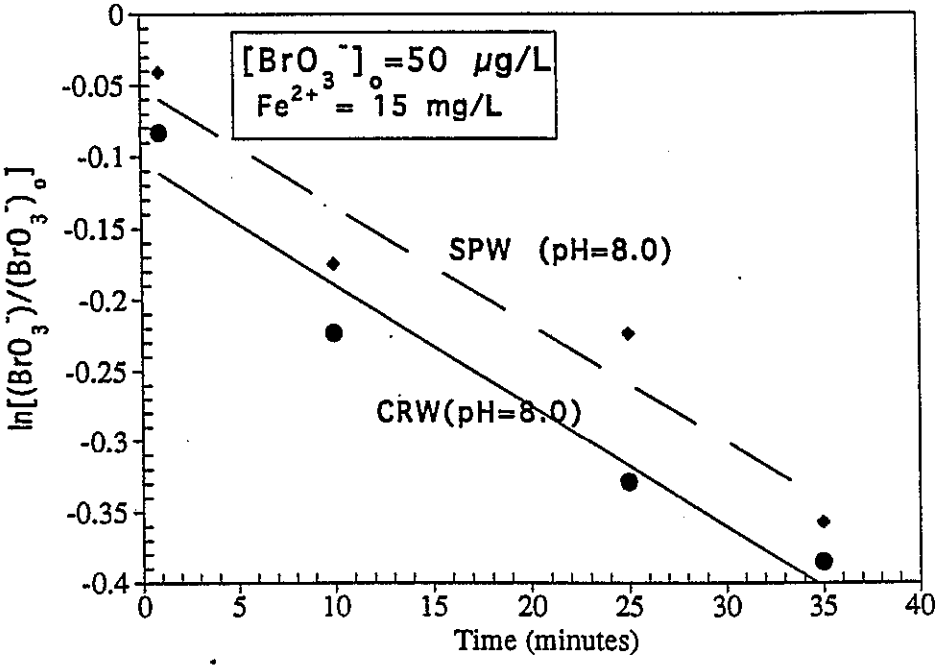

Figure 4.8. First Order Kinetics of Bromate Reduction By Fe^{2+}

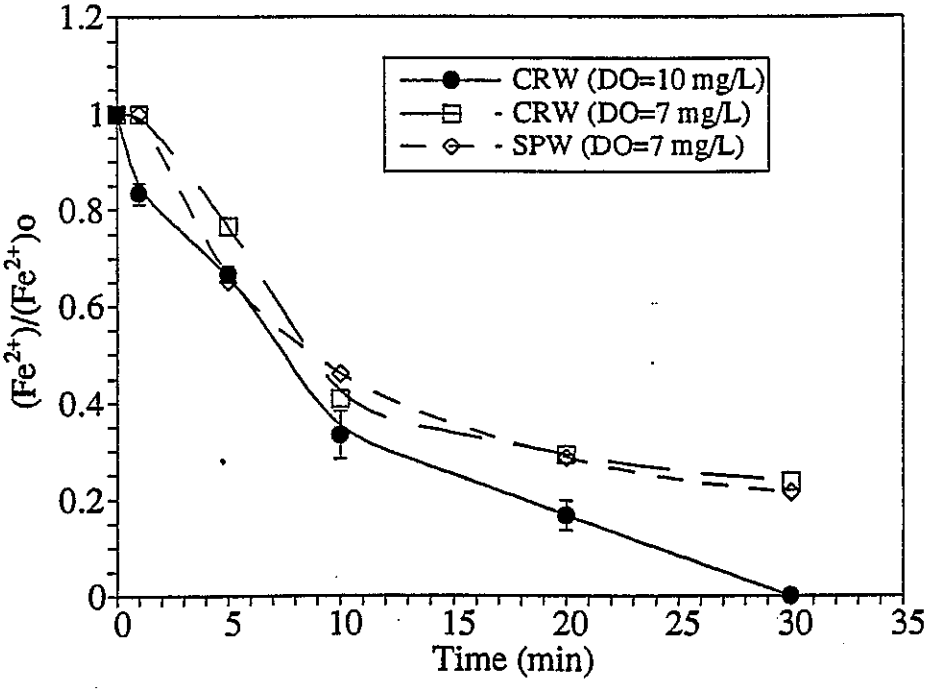

Figure 4.9. Effects of DO on the Disappearence of Fe^{2+} in Source Waters

equation [4.5] at different experimental conditions for BrO_3^- reduction by Fe^{2+} are summarized in Table 4.2 for some source waters.

Table 4.2. Effect of Fe^{2+} Dose and pH on k' for BrO_3^- Reduction

Source Water	Fe^{2+} mM	Initial pH	$[BrO_3^-]_o$ μM	k' min^{-1}
MQW	0.531	6.5	0.392	0.112
MQW	0.531	8.0	0.392	0.061
SLW	0.086	7.5	0.392	0.008
SLW	0.172	7.5	0.392	0.011
SLW	0.261	7.5	0.392	0.025
SPW	0.261	8.0	0.392	0.011
CRW	0.261	8.0	0.193	0.015
CRW	0.261	8.0	0.392	0.014
CRW	0.261	8.0	0.591	0.013

4. Effect of Dissolved Oxygen. The effect of DO concentration on BrO_3^- removal and Fe^{2+} kinetics in CRW was evaluated at 7, and at 10 mg/l DO by sparging with pure oxygen. Measurements made after coagulation showed better DOC removal at higher DO levels and slightly impaired BrO_3^- removal since conversion of Fe^{2+} to Fe^{3+} was faster at higher DO levels. Under ambient DO conditions, BrO_3^- reduction kinetics were largely unaffected (see Figure 4.9) over the range tested. This is because according to equation (1), the stochiometric amount of Fe^{2+} required to reduce BrO_3^- to Br^- is only 6:1 but Fe^{2+} was present in excess of this ratio (50 times more than the stochiometric ratio). The ferrous reduction experiments were performed primarily in water with ambient dissolved oxygen levels of approximately 7 mg/L. However, after ozonation, DO levels could be as high as 15-20 mg/L.

5. Effect of Time. The kinetics of of BrO_3^- reduction are relatively faster than the kinetics of Fe^{2+} oxidation by DO (equation 4.2), and are strongly dependent on Fe^{2+} dose and pH [equation 4.5, Table 4.2]. In general, the majority of the BrO_3^- reduction occurred in less than 10 minutes and appeared to reach equilibrium within 15 minutes. During this kinetic study, the coagulation protocol explained in the experimental section was not precisely followed to investigate the reduction of BrO_3^- over a 0-30 minutes time-frame. Figure 4.10 shows an arithmetic plot of the variation of BrO_3^- with time for SLW (at constant pH of 7.5). Also, over 65% of Fe^{2+} added was converted to Fe^{3+} in less than 30 minutes in both SPW and CRW source waters at ambient pH and DO levels (DO $\approx$ 7 mg/L) (Figure 4.7). These kinetics demonstrate that BrO_3^- reduction is feasible within a flocculation basin, with a typical hydraulic residence time (HRT) of about 30 minutes. First order kinetics for Fe^{2+} disappearance were found to be

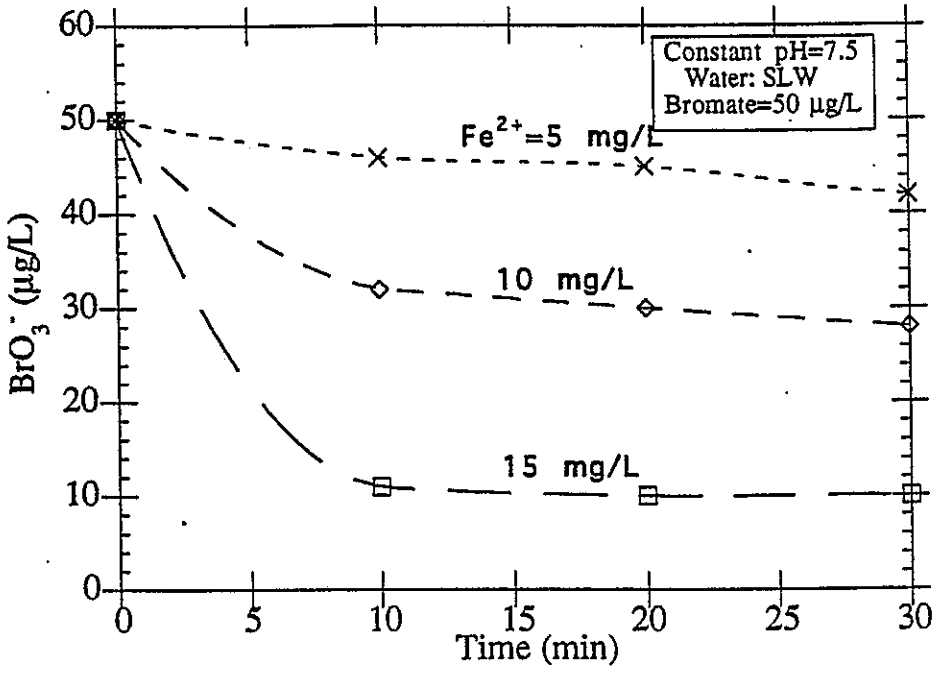

Figure 4.10. Effects of Fe^{2+} Dose and Time on Bromate Reduction

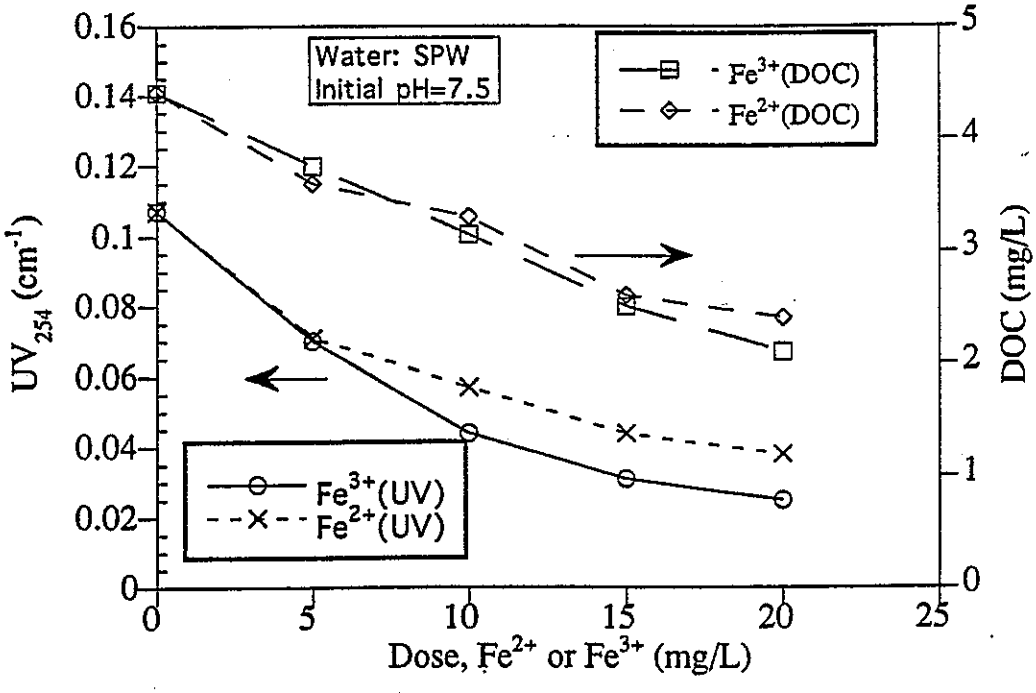

Figure 4.11. Comparison of Fe^{2+} and Fe^{3+} For DOC and UV Absorbance Reduction

a little faster for CRW than SPW because of the higher alkalinity (same DO levels). Fe^{2+} persisted in its dissolved state in SLW for a longer time than SPW and CRW because of very low alkalinity ($Alkalinity_{SLW} < 15$ mg/L $CaCO_3$) and relatively similar dissolved oxygen level (BrO_3^- reduction kinetics were favored at lower alkalinities). The stoichiometry of Fe^{2+} addition to reduce BrO_3^- to Br^- according to equation (1) is 6:1, yet 20 mg/L of Fe^{2+} only reduced up to 40% of the initial BrO_3^- when Fe^{2+} was present at 50 times more than the stochiometric ratio. This indicates that dissolved oxygen, DOC, and alkalinity are collectively competing with BrO_3^- for available Fe^{2+}.

6. Dissolved Organic Matter (DOC) Removal. Figure 4.11 shows the effect of adding comparable amounts (equivalent in terms of weight) of Fe^{2+} and Fe^{3+} salts to the SPW source on DBP precursor removals, as indicated by DOC removal and UV absorbance reductions at ambient pH levels (7.5). Addition of the Fe^{2+} provided slightly less UV_{254} absorbance removal than the Fe^{3+} salt, while comparable DOC removals were observed. Thus, Fe^{2+} salts can provide effective DOC removal while reducing BrO_3^-.

7. Effect of Temperature. The effect of temperature on BrO_3^- reduction kinetics by ferrous coagulation was evaluated at three different temperatures (10, 15, and 20 °C). Reduction of BrO_3^- to Br^- at 10 °C was almost 50% lower than at 20 °C presumably due to accelerated reaction kinetics at higher temperatures (Figure 4.12).

The temperature dependency of the rate constant can be represented by the following Arrehenius law [R= gas constant (cal/mol/K), T = absolute temperature (K), A = frequency factor = 584 min^{-1}].

$$k = Ae^{-6098/RT} \qquad [4.6]$$

The temperature rise needed to double the rate of $BrO3^-$ reduction for an activation energy of 6098 cal/mole at an average temperature of 288 K is estimated to be 289 K (16 °C). The magnitude of activation energy determined indicates that BrO_3^- reduction by Fe^{2+} is temperature sensitive.

Effect of Initial Bromate. Because of the low initial BrO_3^- concentrations used (compared to Fe^{2+} doses used), initial BrO_3^- concentration had no apparent effect on BrO_3^- reduction kinetics (Figures 4.13 and 4.14).

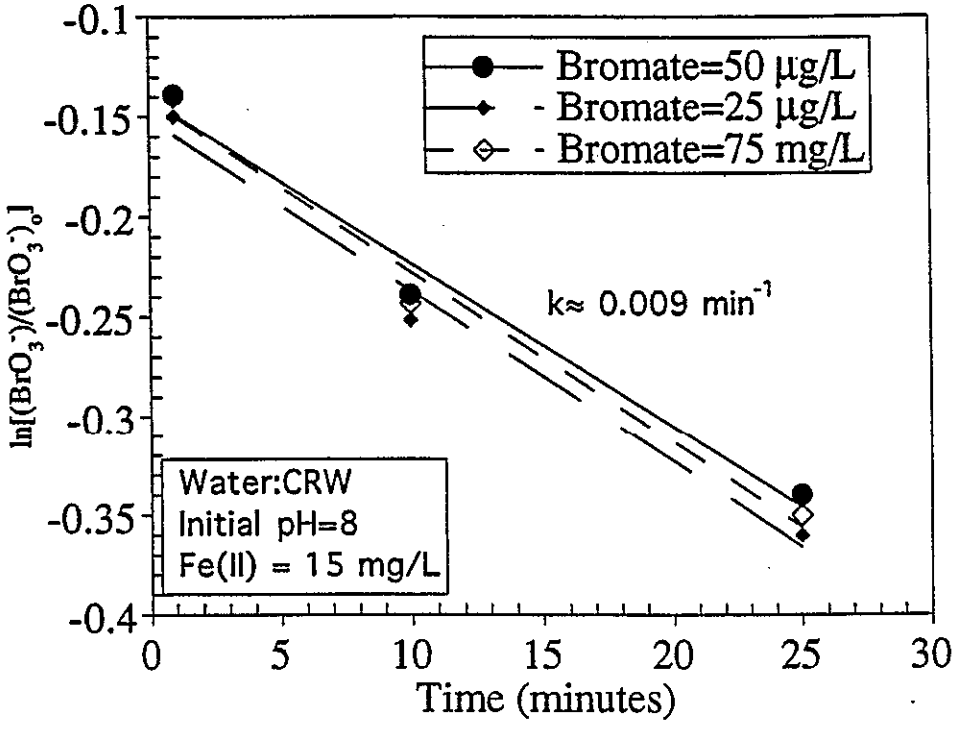

Figure 4.14. Effect of Initial Bromate on Bromate Reduction

Conclusions

The reduction of bromate is dependent upon pH, alkalinity, DOC, temperature and dissolved oxygen of the source water and is apparently independent of the initial bromate concentration. Most of bromate reduction occurs in less than 10 minutes and the use of a ferrous salt for both bromate reduction and DOC removal is feasible.

Complete data for bromate reduction by ferrous iron is given in Tables 4.3-4.13.

Table 4.3. Effect of pH and Iron Dose on Bromate Reduction (CRW)

$FeSO_4.7H_2O$, mg/L	BrO_3^-, µg/L	Initial pH	Final pH	% BrO_3^- Reduction
20	50	6.5	6.5	2
30	50	6.5	6.4	16
40	50	6.5	6.3	20
50	50	6.5	6.3	37
100	50	6.5	—	90
20	50	7.5	7.3	2
30	50	7.5	7.1	6
40	50	7.5	7.0	15
50	50	7.5	6.9	25
100	50	7.5	—	65
20	50	8.5	7.9	0
30	50	8.5	7.8	5
40	50	8.5	7.5	12
50	50	8.5	7.3	18
100	50	8.5	—	50

Table 4.4. Effect of Initial Bromate and Ferrous Dose on Bromate Reduction (CRW): Ambient pH

$FeSO_4.7H_2O$ mg/L	BrO_3^- µg/L	Initial pH	Final pH	% UVA Reduction	% BrO_3^- Reduction
25	25	8.2	7.5	35	5
50	25	8.2	7.2	25	20
75	25	8.2	6.9	25	40
100	25	8.2	6.6	23	60
25	50	8.2	7.5	35	7
50	50	8.2	7.2	25	19
75	50	8.2	6.9	25	31
100	50	8.2	6.6	23	52
25	75	8.2	7.5	35	4
50	75	8.2	7.2	25	10
75	75	8.2	6.9	25	20
100	75	8.2	6.6	23	40

Table 4.5. Effect of pH and Iron Dose on Bromate Reduction (SPW)

$FeSO_4.7H_2O$ mg/L	BrO_3^- µg/L	Initial pH	Final pH	% BrO_3^- Reduction
30	50	6.5	6.5	10
60	50	6.5	6.4	30
80	50	6.5	6.2	40
100	50	6.5	6.2	55
30	50	7.5	6.9	8
60	50	7.5	6.7	26
80	50	7.5	6.7	32
100	50	7.5	6.6	38
30	50	8.5	7.2	0
60	50	8.5	7.1	8
80	50	8.5	6.9	20
100	50	8.5	6.7	32

Table 4.6. Effect of Initial Bromate and Iron Dose on Bromate Reduction (SPW): Ambient pH

$FeSO_4.7H_2O$ mg/L	BrO_3^- µg/L	Initial pH	Final pH	% UVA Reduction	% BrO_3^- Reduction
25	25	7.9	7.1	34	4
50	25	7.9	6.7	44	12
75	25	7.9	6.5	50	20
100	25	7.9	6.3	52	36
25	50	7.9	7.1	34	10
50	50	7.9	6.7	44	15
75	50	7.9	6.5	50	25
100	50	7.9	6.3	52	36
25	75	7.9	7.1	34	7
50	75	7.9	6.7	44	18
75	75	7.9	6.5	50	27
100	75	7.9	6.3	52	40

Table 4.7. Effect of pH and Iron Dose on Bromate Reduction (SPW-II)

$FeSO_4.7H_2O$ mg/L	BrO_3^- µg/L	Initial pH	Final pH	% UVA Reduction	% BrO_3^- Reduction
20	30	6.5	6.5	13	36
40	30	6.5	6.3	26	46
60	30	6.5	6.1	56	81
80	30	6.5	6.0	62	100
20	30	7.5	7.4	13	35
40	30	7.5	7.3	26	39
60	30	7.5	7.2	56	66
80	30	7.5	7.0	62	84
20	30	8.5	8.3	13	29
40	30	8.5	7.9	26	36
60	30	8.5	7.7	56	47
80	30	8.5	7.5	62	64

Table 4.8. Effect of pH and Iron Dose on Bromate Reduction (ACW)

$FeSO_4.7H_2O$ mg/L	BrO_3^- µg/L	Initial pH	Final pH	% UVA Reduction	% BrO_3^- Reduction
25	50	6.5	6.5	32	18
50	50	6.5	6.4	38	52
75	50	6.5	6.3	64	78
100	50	6.5	6.3	76	100
25	50	7.5	7.4	32	14
50	50	7.5	7.2	38	30
75	50	7.5	7.0	64	54
100	50	7.5	6.8	76	64
25	50	8.5	7.6	32	20
50	50	8.5	7.4	38	24
75	50	8.5	7.2	64	54
100	50	8.5	7.0	76	68

Table 4.9. Effect of Iron Dose and Bromate on Bromate Reduction (ACW)

$FeSO_4.7H_2O$ mg/L	BrO_3^- µg/L	Initial pH	Final pH	% UVA Reduction	% BrO_3^- Reduction
25	25	7.5	7.3	32	8
50	25	7.5	7.1	40	20
75	25	7.5	6.9	62	36
100	25	7.5	6.7	69	52
25	50	7.5	7.3	32	14
50	50	7.5	7.1	40	29
75	50	7.5	6.9	62	50
100	50	7.5	6.7	69	64
25	75	7.5	7.3	32	8
50	75	7.5	7.1	40	13
75	75	7.5	6.9	62	27
100	75	7.5	6.7	69	50

Table 4.10. Effect of pH and Iron Dose on Bromate Reduction (CCW)

$FeSO_4.7H_2O$ mg/L	BrO_3^- µg/L	Initial pH	Final pH	% UVA Reduction	% BrO_3^- Reduction
25	50	6.5	6.5	25	20
50	50	6.5	6.4	70	28
75	50	6.5	6.3	85	44
100	50	6.5	6.3	85	58
25	50	7.5	7.4	25	12
50	50	7.5	7.2	70	34
75	50	7.5	7.0	85	44
100	50	7.5	6.8	85	52
25	50	8.5	7.6	25	6
50	50	8.5	7.4	70	18
75	50	8.5	7.2	85	36
100	50	8.5	7.0	85	54

Table 4.11. Effect of Initial Bromate and Iron Dose on Bromate Reduction (CCW): Ambient pH

$FeSO_4.7H_2O$ mg/L	BrO_3^- µg/L	Initial pH	Final pH	% BrO_3^- Reduction
25	25	7.6	7.4	12
50	25	7.6	7.2	25
75	25	7.6	7.0	40
100	25	7.6	6.8	48
25	50	7.6	7.4	8
50	50	7.6	7.2	25
75	50	7.6	7.0	36
100	50	7.6	6.8	48
25	75	7.6	7.4	12
50	75	7.6	7.2	23
75	75	7.6	7.0	39
100	75	7.6	6.8	45

Table 4.12. Effect of pH and Iron Dose on Bromate Reduction (CCW-II)

$FeSO_4.7H_2O$ mg/L	BrO_3^- µg/L	Initial pH	Final pH	% BrO_3^- Reduction
20	15	6.5	6.5	15
40	15	6.5	6.3	40
60	15	6.5	6.1	78
80	15	6.5	6.0	87
20	15	7.5	7.3	5
40	15	7.5	7.2	20
60	15	7.5	7.2	30
80	15	7.5	7.0	55
20	15	8.5	8.0	4
40	15	8.5	7.8	14
60	15	8.5	7.7	25
80	15	8.5	7.5	45

Table 4.13. Effect of pH and Iron Dose on Bromate Reduction (CCW-II)

$FeSO_4.7H_2O$ mg/L	BrO_3^- µg/L	Initial pH	Final pH	% UVA Reduction	% BrO_3^- Reduction
20	30	6.5	6.5	15	30
40	30	6.5	6.3	30	34
60	30	6.5	6.1	40	55
80	30	6.5	6.0	55	90
20	30	7.5	7.3	15	23
40	30	7.5	7.2	30	34
60	30	7.5	7.2	40	39
80	30	7.5	7.0	55	69
20	30	8.5	8.0	15	25
40	30	8.5	7.8	30	29
60	30	8.5	7.7	40	37
80	30	8.5	7.5	55	61

Part V

Bromate Removal by Activated Carbon (After Intermediate Ozonation)

Not all utilities contemplating ozone application intend to employ pre-ozonation but rather may use intermediate ozonation prior to the filtration process. Apart from Fe^{2+} reduction, removal is possible by activated carbon and UV irradiation. This approach has potential relevance to integration of GAC columns into a process train or, more realistically, to retrofitting of rapid sand filters with GAC-capped filters (replacing anthracite coal with GAC in a conventional filter). Alternatively, after chemical pre-treatment for turbidity and organic matter removal, UV irradiation can potentially be used for both BrO_3^- removal and disinfection.

Characteristics of Different Activated Carbons

Studies were conducted to examine both powdered activated carbon (PAC) and granular activated carbon (GAC) applications. The extent of BrO_3^- adsorption/reduction was found to vary significantly from carbon to carbon, ranging from 20% to 80% removal (Figure 5.1). BrO_3^- removal capacities for different activated carbons were found to vary from 0.02 to 0.45 mg BrO_3^-/g of carbon under PAC application conditions (Table 5.1).

Table 5.1. Inorganic Constituents and Bromate Removal Capacities of Different Carbons

Carbon	Titanium (ppm)	Vanadium (ppm)	Strontium (ppm)	Barium (ppm)	Zirconium (ppm)	Sulfur (ppm)	Iron (ppm)	Capacity^	Rating@
D-10	59	3.7	58	44	4	2000	2090	0.43	1
D-10**	58	3.9	39	43	4	2200	2060	0.45	1
CX0655	63	1	13	50	3	1300	340	0.22	2
F-400	290	23	131	100	10	8000	2900	0.13	3
F-400*	372	22	141	100	10	7000	5100	0.12	3
BL	313	24	128	110	11	7000	4050	0.12	3
WPH	350	31	118	108	12	5900	5800	0.12	3
HDB	1010	35	615	708	60	8000	13300	<0.1	4

* Regenerated GAC
** Acid washed PAC
^ Reduction capacity = mg BrO_3^-/g PAC
@ 1-Best and 4-Worst with respect to BrO_3^- reduction

Chemistry of Bromate Reduction

The inorganic composition of carbon was found to be an important factor in its ability to inhibit surface reduction of BrO_3^- (Table 5.1). An inverse trend was

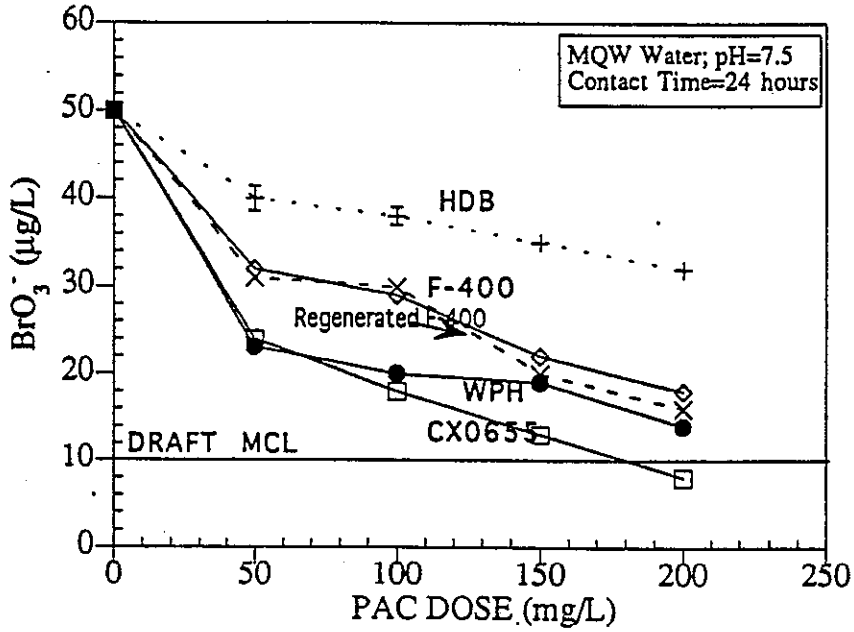

Figure 5.1. Effects of PAC Dose and PAC Type on Bromate Reduction

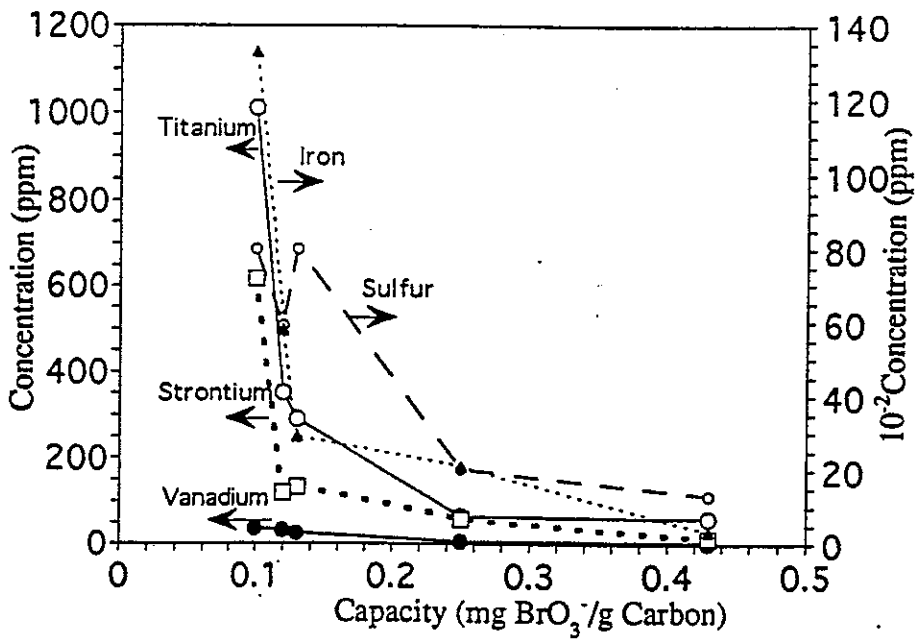

Figure 5.2. PAC Metal Concentration and BrO_3^- Removal Capacities

observed between the carbon content of various catalysts and BrO_3^- reduction capacities of different activated carbons (Figure 5.2). The carbons with least amounts of these metals as well as iron and sulfur showed the highest BrO_3^- removal capacity suggesting that these metals are acting as inhibitors and not catalysts for BrO_3^- reduction. To further substantiate this, concentration of these metals on the surface of different PACs ($\leq$ 25 μm from surface) was measured by an electron microprobe and similar trends were observed. This can attributed to blockage of active surface groups by these metal oxides. Central to the carbon surface reduction of BrO_3^- is the role of carbon surface functional groups present on all activated carbons (-SH (sulfides), -S-S (disulfide like pyrite), $-CO_2OH$ (carbonates)). The functional groups on the surface may depend on the mineral constituents of PAC. Deprotonated surface groups may behave as Lewis bases and their interaction with protons and metal constituents can be understood as competitive complex formation. Similarly, the central ions of the carbon surface can exchange functional groups for other ligands. Thus, the surface of an activated carbon can be considered, in a statistical approach, as a polymeric acid (or base) which undergoes coordination reactions; these reactions may include redox reactions with (surface) coordinated reductants. BrO_3^- reduction on the surface of activated carbon may be represented by complex formation involving a bridging ligand X (our hypothesis is that there is a two-step process; adsorption followed by reduction).

$$\underset{\text{Adsorption}}{[>AX^+] + BrO_3^- \Leftrightarrow [>AX^+BrO_3^-] \Leftrightarrow [>AXOBr] + O_2} \Rightarrow \underset{\text{Reduction}}{BrO^- + [>AX^+]}$$

Further reduction of BrO^- on the surface of activated carbon occurs leading to the formation of Br^-.

The chemical characteristics obtained from analysis of the acid-base titration are presented first for virgin carbons and then for acid washed and regenerated carbon (Table 5.2). The indicated categories of surface chemical groups are classified according to their acid-base character. Groups which are neutral in the acid-base reactions cannot be detected using this method. Carbon D-10 was found to possess much higher number of basic groups ([>AX^+]) than HDB carbon. This is consistent with bromate removal results. Acid washing by 5N nitric acid did not change the number of total basic sites. On the other hand acid washing by 5N HCl increased the number of basic groups and decreased the total number of acidic and carboxylic sites. The ability of carbon to remove bromate was correlated with the number of basic groups on the surface of the activated carbon.

Table 5.2. Acid and Basic Groups of Different Activated Carbons

Carbon	D-10	D-10@	D-10*	HDB	F-400	F-400^	PK
Acid Groups (meq/100g carbon)	23	17	25	80	30	34	24
Basic Groups (meq/100g carbon)	64	84	63	12	60	45	60
Carboxyl + Lactonic Groups (meq/100g carbon)	15	12	18	45	26	31	13
Carboxyl Groups (meq/100g carbon)	5	4	7	30	15	20	4

@ 5N hydrochloric acid washed carbon
* 5N nitric acid washed carbon
^ regenerated carbon

Experimental Matrix. The experimental matrix and ranges of variables studied for bromate removal by activated carbon in different source waters is shown in Table 5.3 for batch experiments and Table 5.4 for RSSCT experiments.

Batch PAC Experiments

Effect of pH. In general, removal of BrO_3^- was found to increase upon lowering pH from 8.0 to 6.0 for carbons D-10, WPH, HDB and F-400, while pH had no significant effect on the CX0655 carbon (Figure 5.3). For most carbons investigated, the charge at high pH values is negative, which corresponds to the presence of negatively charged carboxylate anionic surface functional groups on the carbon. As the pH is lowered, the weakly acidic functional groups are protonated, resulting in a positive change in zeta potential, until the isoelectric point (or point of zero charge) is reached. As pH is lowered, basic groups impart a positive charge. The pH of the isoelectric point varies according to the types and concentrations of acidic/basic functional groups (Figure 5.4; Table 5.2). Activated carbon HDB is more negatively charged and repulsive to bromate than carbon D-10. Continued addition of H^+ ions, after reaching the isoelectric point increases the positively charged sites on the carbon surface.

Similar to the coagulation experiments, Br^- analysis showed that surface reduction of BrO_3^- to Br^- was occurring, presumably through a preliminary transient adsorption step.

Kinetics. Some carbons, in PAC form, provided effective but kinetically slow removal of BrO_3^-. BrO_3^- removals by four different carbons were determined at 4, 24, and 48 hour contact times after adding carbon to solutions containing BrO_3^-. BrO_3^- removal increased from 4 hours to 48 hours (Figure 5.5).

Table 5.3. Experimental Matrix for PAC Batch Experiments

Sources	Carbon Types	pH	PAC dose mg/L	Contact time	Temp °C	BrO_3^- range µg/L
CRW	D-10*, F-300 F-400#, PK	6.0, 7.0, 8.0	25, 50, 75 100	30 min - 24 hrs	20	25-100
SPW	D-10, F-300 F-400, PK	6.0, 7.0, 8.0	25, 50, 75 100	10 min - 24 hrs	20	25-100
ACW	D-10, F-300 F-400, PK	6.0, 7.0, 8.0	25, 50, 75 100	30 min - 24 hrs	20	25-100
SLW	D-10, F-300 F-400, PK	6.0, 7.0, 8.0	25, 50, 75 100	10 min - 24 hrs	20	25-100
MQW	D-10, F-300 F-400, PK	6.0, 7.0, 8.0	25, 50, 75 100	10 min - 24 hrs	20	25-100
CCW	D-10, F-300 F-400, PK	6.0, 7.0, 8.0	25, 50, 75 100	30 min - 24 hrs	20	25-100

* both virgin and acid washed carbons were evaluated
# both virgin and regenerated carbons were evaluated

Table 5.4. Experimental Matrix for RSSCT Experiments

Source	F-400		F-300		PK	
	pH=6.0	pH=amb	pH=6.0	pH=amb	pH=6.0	pH=amb
SPW	√	√[1]	√	√	√	--
CCW	√	√[2]	--	--	--	√
ACW	--	--	--	√	--	--
LAW	√	√	√	--	--	√
SLW	√	√	√[3]	--	--	--
MQW	√	--	√	--	--	--

[1] three different EBCT's [5, 10, 20 min] evaluated
[2] two different EBCT's [4, 10 min] evaluated
[3] two different EBCT's [5, 10 min] evaluated

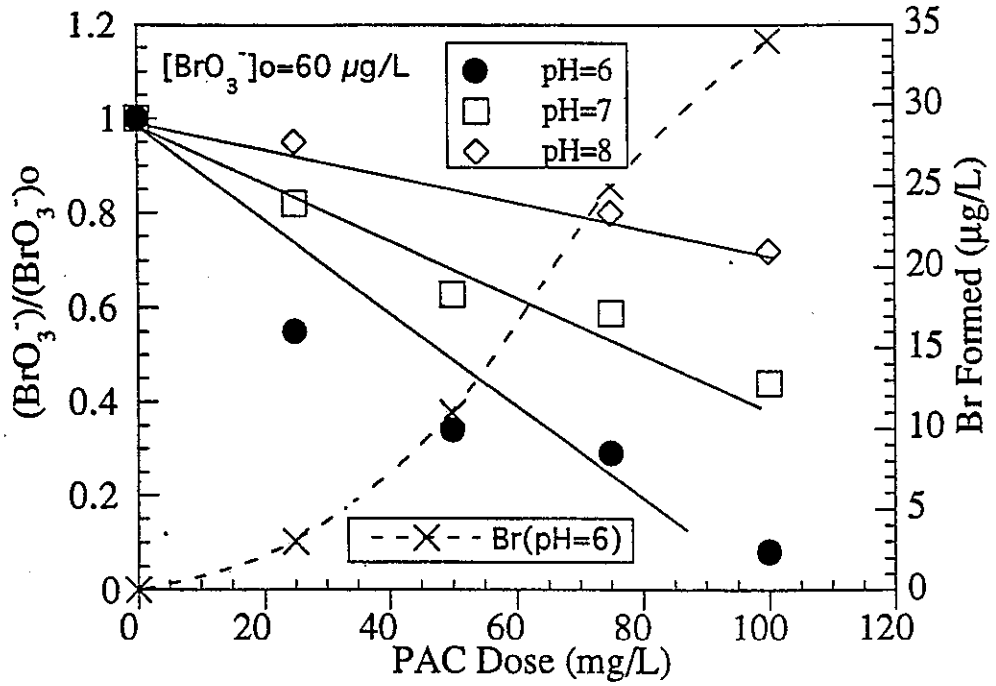

Figure 5.3. Effects of pH on Bromate Reduction by PAC (D-10, SPW)

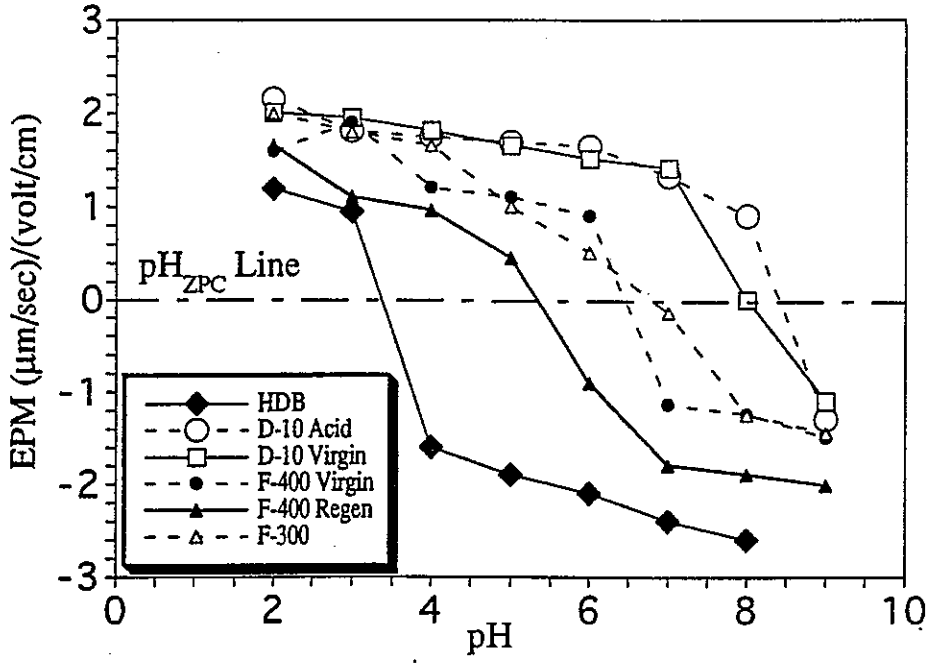

Figure 5.4. Isoelectric Points of Different Activated Carbons

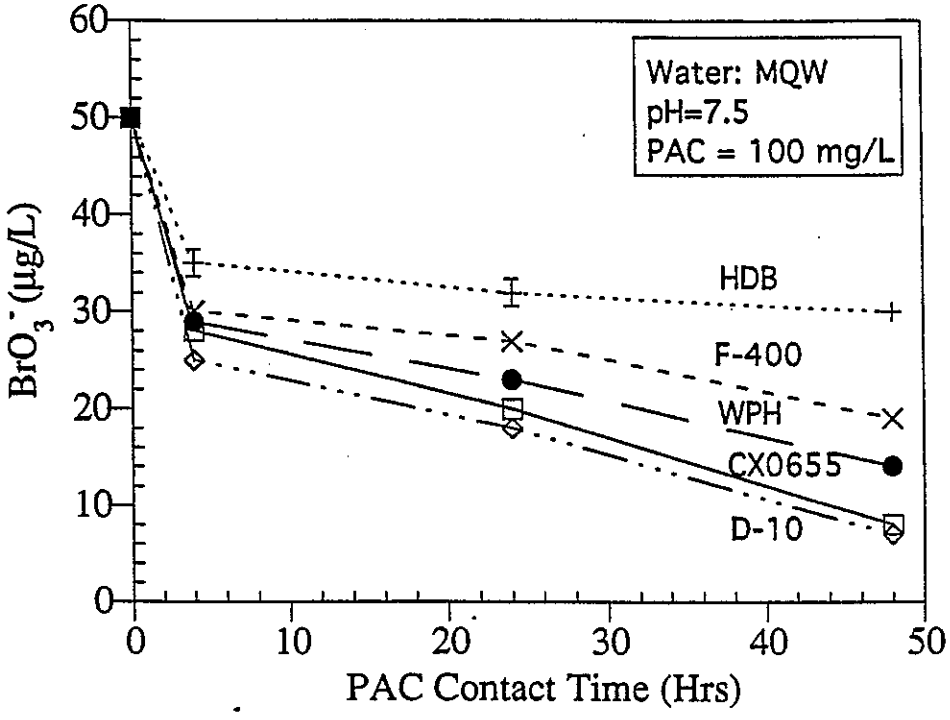

Figure 5.5. Effect of PAC Contact Time on Bromate Reduction

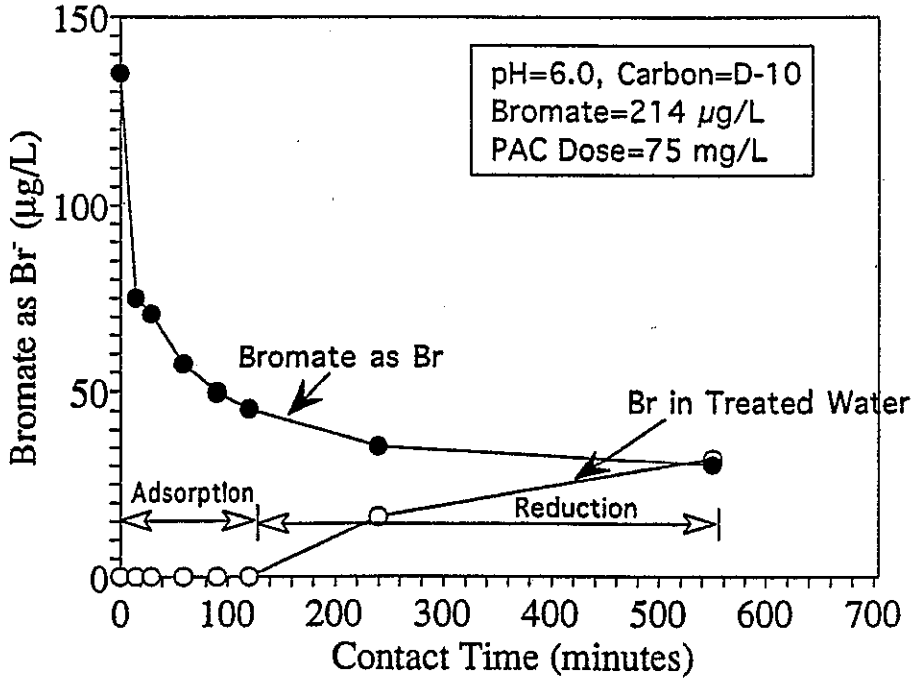

Figure 5.6. Bromate Reduction and Br Formation

However, most of the reduction occurred within 4 hours of PAC contact time. When carbon D-10 was used, 50% of the BrO_3^- removal occurred in less than 15 minutes (Figure 5.6). Prados et al. (1993) have reported over 80% of removal within 10 hours using coconut-based activated carbons. Because of contact time requirments, PAC does not seem the appropriate technique to remove BrO_3^- unless an appropriate PAC is employed and sufficient dosages are used.

Effect of DOC. Waters containing DOC concentrations ranging from 0.15 to 4 mg/L were evaluated for BrO_3^- reduction to see if background organic matter (NOM) would compete with BrO_3^- for active sites on the carbon, or whether adsorbed NOM would mask potential surface reduction sites. MQW water with a DOC of 0.15 mg/L showed the highest BrO_3^- removal when compared with other source waters (Figure 5.7). Thus, NOM appears to compete for, or mask active sites. This also indicates that source waters with moderate to high DOC levels can expect poorer BrO_3^- removal as a result of competition for the carbon adsorption sites.

Effect of Acid Washing. BrO_3^- removal efficiencies were compared using PAC with and without acid washing with 0.1 M HCl. BrO_3^- removal was significantly enhanced by acid washing PAC, presumably due to activation of inactive sites and removal of surface impurities; this is shown at two different pH levels (8.0 and 6.0) for carbon D-10 (Figure 5.8). Thus, acid washing affects the surface chemistry of the carbon, enhancing BrO_3^- reduction. The analysis of PAC after extraction with acid showed almost 50% reduction in ash content and the amount of surface complex on the activated carbon seems to be greatly increased by the extraction process. BrO_3^- reductions by regenerated F-400 activated carbon and virgin F-400 activated carbon were similar indicating that BrO_3^- reduction capacity could be regenerated and/or regeneration does not adversely affect the surface chemistry responsible for BrO_3^- reduction. Analysis for inorganic constituents of the carbon including iron and sulfur after acid washing indicated no change, indicating that acid washing apparently increased the number of active sites for BrO_3^- reduction without changing the chemical composition of PAC. Also high temperature regeneration of GAC did not change the concentration of metals on the surface of the carbon. Prados et al. (1993) compared the removal of bromate using virgin and saturated (spent) coconut-based activated carbon and noted that saturated GAC removed only up to 40% as compared to 100% removal using virgin GAC.

Temperature. Temperature had a significant effect on BrO_3^- removal by PAC. BrO_3^- removal increased on increasing temperature from 10 to 20 ^oC

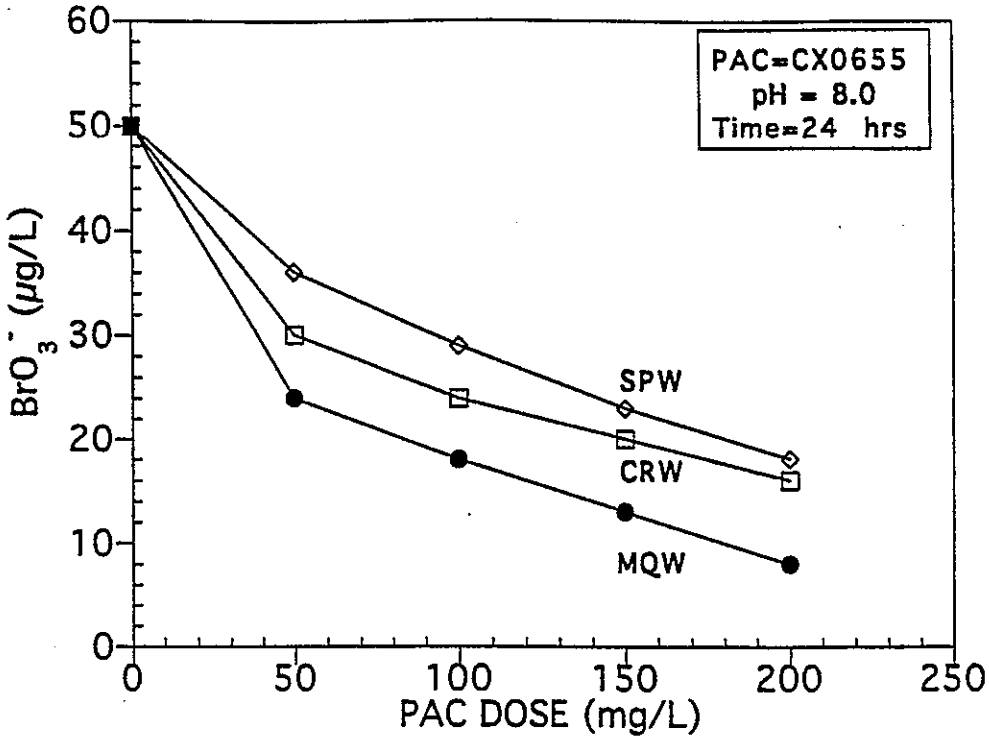

Figure 5.7. Effect of Background DOC on Bromate Reduction By PAC

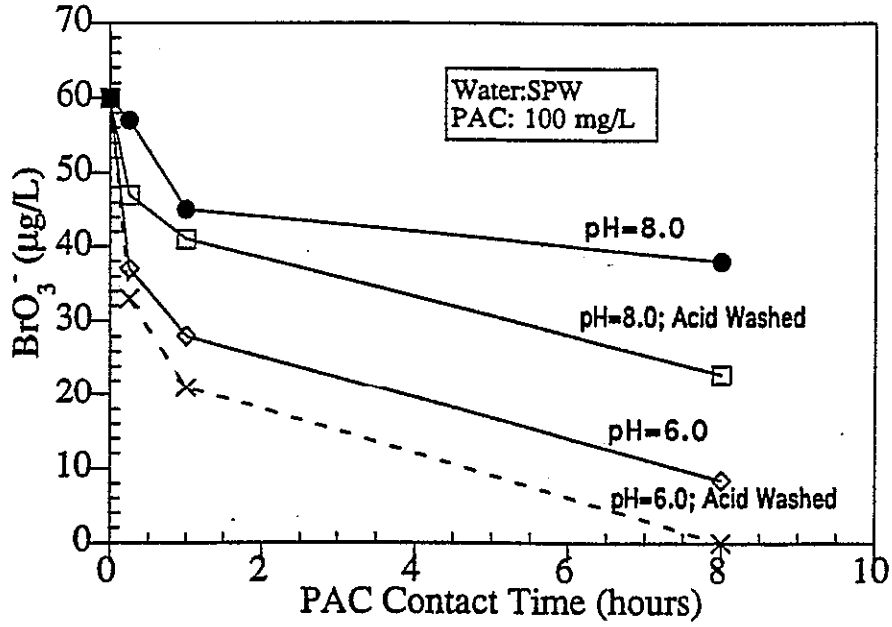

Figure 5.8. Effects of Acid Washing on BrO_3^- Reduction (D-10)

presumably due to an increase in diffusivity (increasing diffusivity increases the diffusion of solutes into the micropores of the PAC).

Table 5.5 summarizes complete data including final pH levels and Br^- formed for BrO_3^- reduction by PAC for Figures 5.3 and 5.6. These data supports the theory that adsorption precedes chemical reduction since not all Br in BrO_3^- is accounted for.

Table 5.5. Bromide Mass Balance for BrO_3^- Reduction By PAC (D-10)

Source Water	Figure #	PAC mg/L	Time	Initial pH	Final pH	% BrO_3^- Reduced	% Br Recovered	% Br Adsorbed
MQW	5.6	75	15 min	6.0	6.1	44	0	100
MQW	5.6	75	30 min	6.0	6.2	47	0	100
MQW	5.6	75	60 min	6.0	5.9	57	0	100
MQW	5.6	75	90 min	6.0	6.3	62	0	100
MQW	5.6	75	120 min	6.0	6.2	66	0	100
MQW	5.6	75	240 min	6.0	6.2	74	25	75
MQW	5.6	75	570 min	6.0	6.2	79	54	46
SPW	5.3	25	24 hr	6.0	6.1	45	22	78
SPW	5.3	50	24 hr	6.0	6.2	67	44	56
SPW	5.3	75	24 hr	6.0	6.3	72	92	8
SPW	5.3	100	24 hr	6.0	6.5	92	100	0

RSSCT Continuous Column Experiments

A rapid method for design of a large-scale fixed bed column from small column studies, known as the rapid small-scale column test (RSSCT), was used to assess GAC. This test procedure dramatically reduces the time and effort necessary to select the conditions necessary for GAC reduction of BrO_3^-. The RSSCT test may be conducted in a fraction of the time required to conduct a pilot study. The RSSCT similitude methodology for constant diffusion is employed to simulate a pilot plant with an EBCT of 10 -15 minutes (Table 2.2). Although the RSSCT column testing scale-up methodology employed may be valid only for the removal of DOC, it can still be used for preliminary evaluations of BrO_3^- removal as long as one keeps this objective in mind.

The RSSCT relies on scaling equations that give a smaller particle size, higher application rate and smaller EBCT than pilot or full scale operation. The time to breakthrough is scaled up according to:

$$[R_{SC}/R_{LC}]^2 = t_{SC}/t_{LC}$$

where R_{SC} is particle size in the small column used in the RSSCT; R_{LC}, the particle size in the large column; t_{SC}, the time to reach any concentration in the small column; and t_{LC}, the time to reach the same concentration in the large column. This relationship holds if the process is limited by internal diffusion and if the diffusion coefficient does not depend on particle size.

Unfortunately, experience with the RSSCT reveals that when NOM adsorption is involved, the diffusion coefficient may depend linearly on particle size, thus changing the scaling relationship to:

$$[R_{SC}/R_{LC}] = t_{SC}/t_{LC}$$

This may yield a large difference in prediction of service time. But since breakthrough of bromate normally occurs later than the breakthrough of NOM, this may not hold true for bromate reduction.

Formation of Bromide. Figure 5.9 shows the breakthrough curves for UV absorbance (an indicator of NOM breakthrough), BrO_3^-, and Br^- (Br^- being produced within the column during BrO_3^- reduction; F-300). In this RSSCT experiment, raw water from SLW was spiked with 50 µg/L of BrO_3^-. UV_{254} absorbance was found to represent DOC well and a gradual breakthrough of organic matter occurred (C/C_O=0.62 after 7500 bed volumes). The BrO_3^- was completely removed in the column initially, and then BrO_3^- levels were found to slowly increase over time after 3,000 bed volumes. A lag in the Br^- appearance in the column effluent suggests that BrO_3^- adsorption onto GAC occurs initially and then adsorbed BrO_3^- undergoes surface reduction. Adsorption and reduction of BrO_3^- occurs and Br^- is removed by diffusion and advective flow.

Effect of Source Water. Figure 5.10 shows BrO_3^- breakthrough curves for SLW and SPW waters. Since the SPW source water is subjected to saltwater intrusion and contained sulfate, chloride and other anions at much higher levels than SLW which may compete with BrO_3^- for adsorption sites; thus, BrO_3^- breakthrough occurred earlier for SPW than SLW. In these experiments, raw untreated source waters were used and the low capacity for BrO_3^- may be attributed to preferential adsorption by the GAC of DOC rather than BrO_3^- and

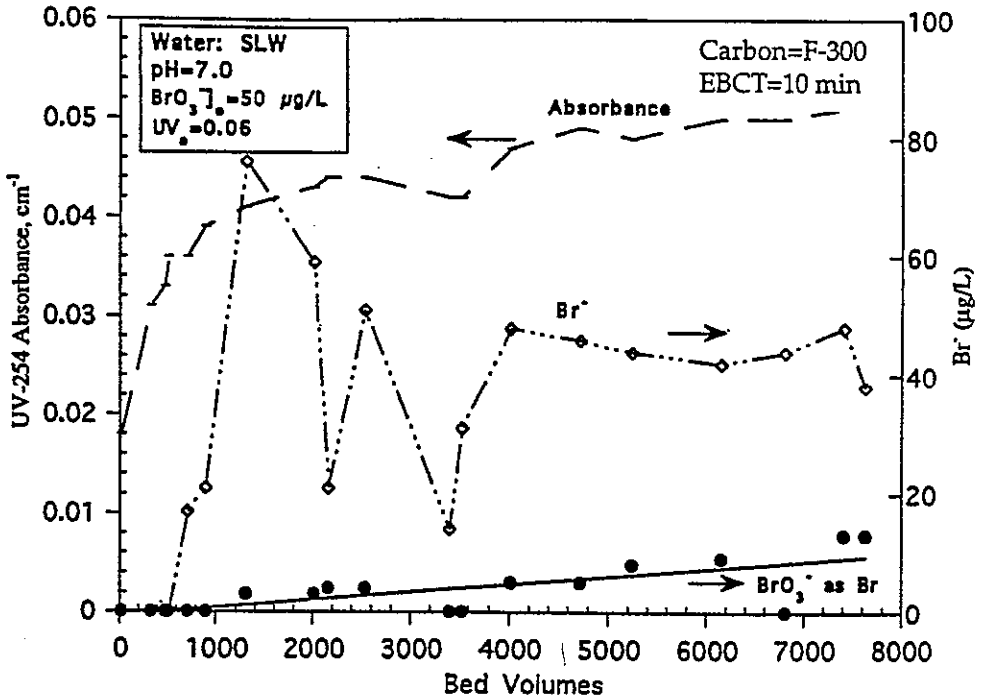

Figure 5.9. RSSCT Breakthrough Curves for UV-Absorbance, BrO_3^-, and Br^-

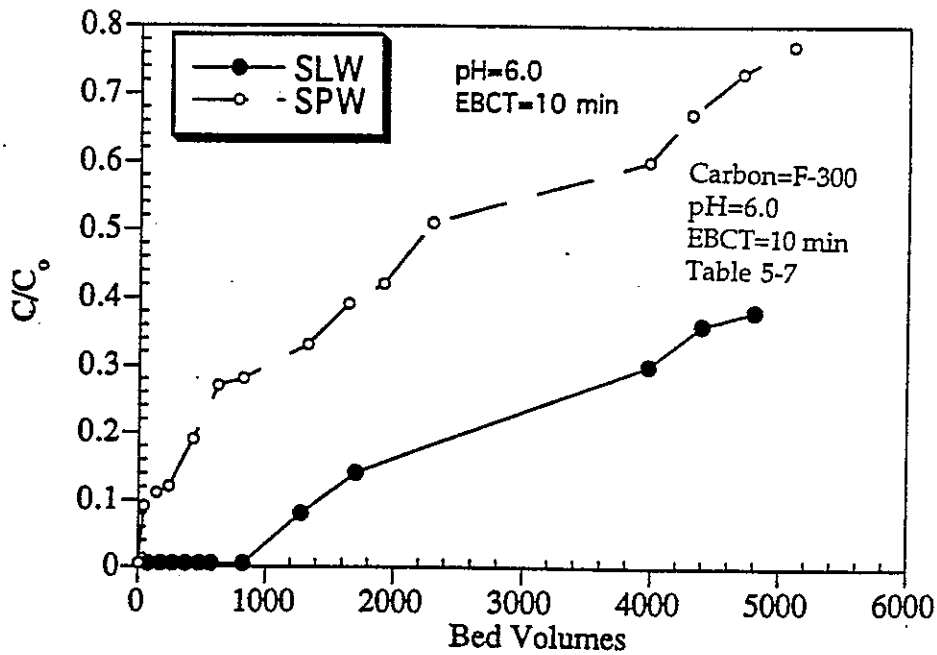

Figure 5.10. Effect of Source Water on Bromate Reduction By GAC

competition from other anions like sulfate. The results suggest that a GAC filter-cap would not be suitable for removing BrO_3^- from untreated SPW water but since a filter cap is used after coagulation, the filter cap would be able to remove BrO_3^- from chemically pretreated SPW for much longer time than raw SPW due to reduction in competition from background organic carbon. The effective life for BrO_3^- removal could be many times that for DOC removal for SLW, and possibly filtered SPW water. Breakthrough for BrO_3^- was never reached even after one week (8,000 bed volumes) for SLW, even though DOC/UV absorbance breakthrough was reached after 4 days for the same source water.

One of the difficulties recognized in use of dynamic models is the inability to describe adsorption between bromate and NOM largely because adsorption characteristics of NOM are not well understood, nor predictable. An alternative approach is to treat NOM as unspecified background matter in solution.The DOC breakthrough behavior affects the BrO_3^- breakthrough profiles for RSSCTs. The blocking of surface groups by large molecular size humic and fulvic acids present in DOC will eventually decrease the BrO_3^- reduction capacity of GAC. Much better removal of BrO_3^- was achieved by GAC using rapid small scale column tests (RSSCT), as compared to using the same carbon in a PAC mode of application. The kinetics of BrO_3^- reduction do not appear to be as limiting in a GAC column mode in comparison to a PAC batch mode of application; significantly higher rates of BrO_3^- removal were observed in the former.

Effect of pH. The effect of varying pH was studied at pH 6 and 8 for CCW and the removal of bromate at pH 6 was significantly greater (Figure 5.11). This is possibly because, for most carbons investigated, the charge at high pH values is negative, which corresponds to the presence of negatively charged carboxylate anionic surface functional groups on the carbon. As the pH is lowered, the weakly acidic functional groups are protonated, resulting in a positive change in zeta potential. Continued addition of H^+ ions after reaching the isoelectric point increases the positively charged sites on the carbon surface. In water treatment decreasing pH to 8 from 6 to enhance bromate removal may not be cost-effective for high alkalinity waters.

Effect of EBCT. The effect of different EBCTs on bromate reduction was evaluated by varying the water flow rate form 10 to 20 ml/min (equivalent EBCT of 4-10 minutes) (Figure 5.12). Increasing flow rates accelerated the breakthrough of bromate through the carbon column. In other words, more effective removal of bromate was observed at lower flow rates and higher contact times.

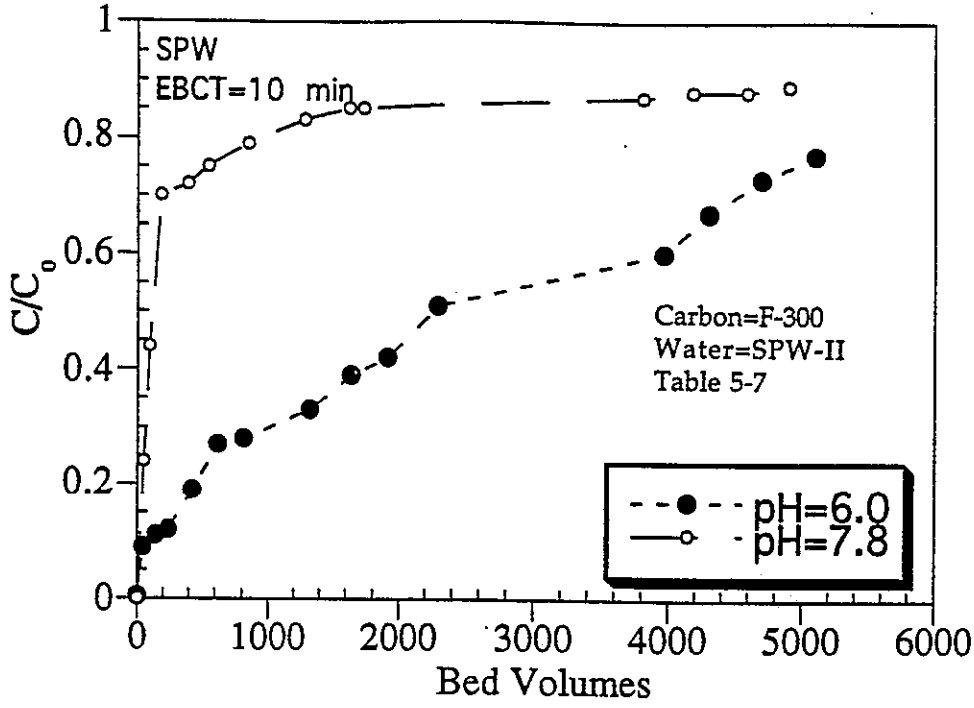

Figure 5.11. Effect of pH on Bromate Reduction

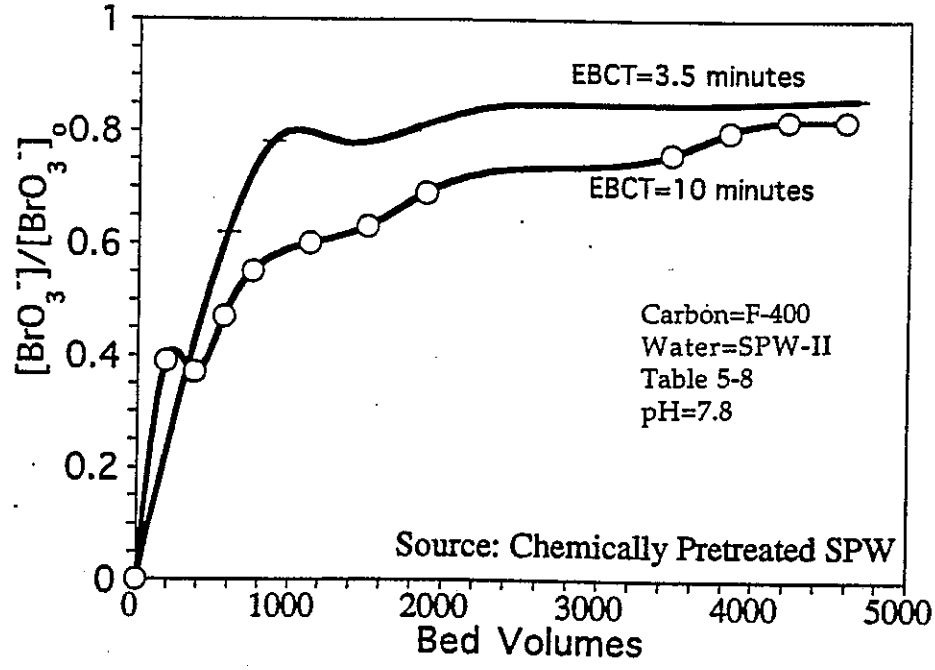

Figure 5.12. Effect of EBCT on Bromate Removal By GAC (F-400)

GAC may be an effective treatment scenario as a filter cap (on top of sand media; EBCT of 3-5 minutes) or a full depth GAC column (EBCT of 10-12 minutes) depending upon the background characteristics of the source water. Variations of EBCT from 3 to 20 minutes were found to comparably reduce BrO_3^- in SLW. Hence, a filter cap scenario may be more effective for low alkalinity and low TDS waters than waters such as SPW and CCSW. Marhaba et al. (1993) reported greater than 90% BrO_3^- removal with an EBCT of 5-10 minutes in pilot-scale experiments. The difference in performance between the bench-scale PAC tests and GAC column tests may be possibly attributed to the overall increased surface contact area per unit volume of water, and turbulent flow conditions which minimize diffusional limitations.

Effect of Carbon Type. Three different activated carbons (F-300, F-400 and PK) with different surface and origin were evaluated and the results are shown in Figures 5.13 and 5.14 for SLW and SPW. Since PK and F-300 carbons have a higher number of basic groups and possesses a higher isoelectricpoint than F-400 carbon, bromate removal by the PK and F-300 carbons was better than by F-400 carbon.

The breakthrough curve reflects the shape of the concentration profile as it exits the carbon bed. Because external and internal diffusion occurs in series, the slowest of these steps controls the overall rate of adsorption and reduction of bromate. The breakthrough curves are steeper because of faster mass transfer and chemical reduction. In some cases, the breakthrough curves were found to rise rapidly and then tend to tail off as the effluent approaches the influent concentration, indicating that internal diffusion is slower.

After one of the RSSCT breakthrough experiments, spent activated carbon was removed from the RSSCT column (8,000 bed volumes) and divided into three aliquots and washed with acid (0.1 M H_2SO_4), MQW water, and base (0.1 M NaOH). No BrO_3^- was found in any of these aliquots but increasing amounts of Br^- were found in the acid, MQW and base washes respectively. Measuring the mass of Br species in the column influent and effluent, 95% of the BrO_3^- reduced to Br^- was accounted for.

Table 5.6 shows bed volumes required to reach 50% breakthrough of bromate for various carbons at different experimental conditions.

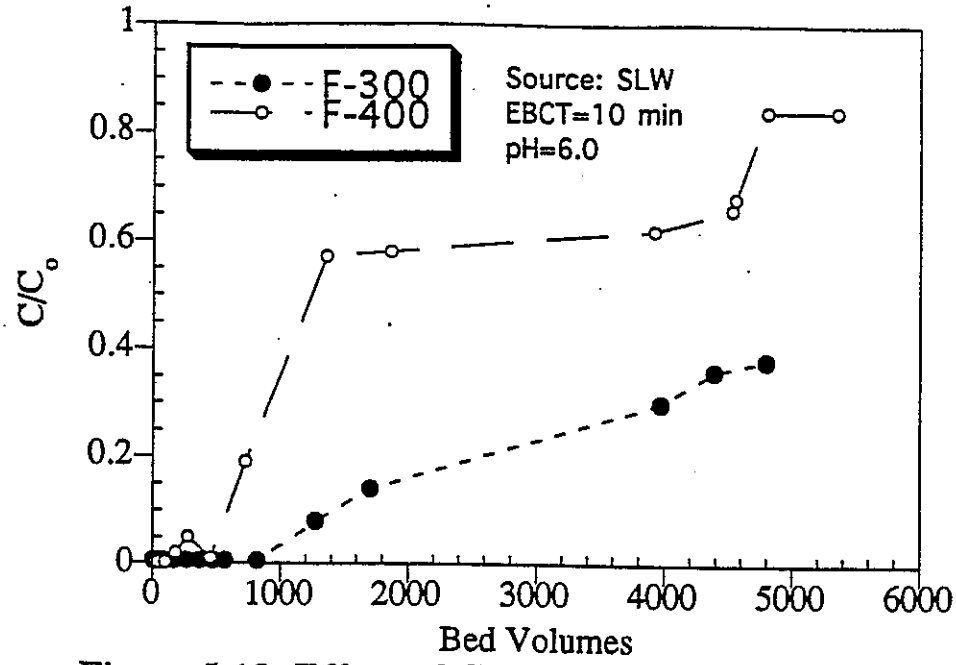

Figure 5.13. Effect of GAC on Bromate Reeduction

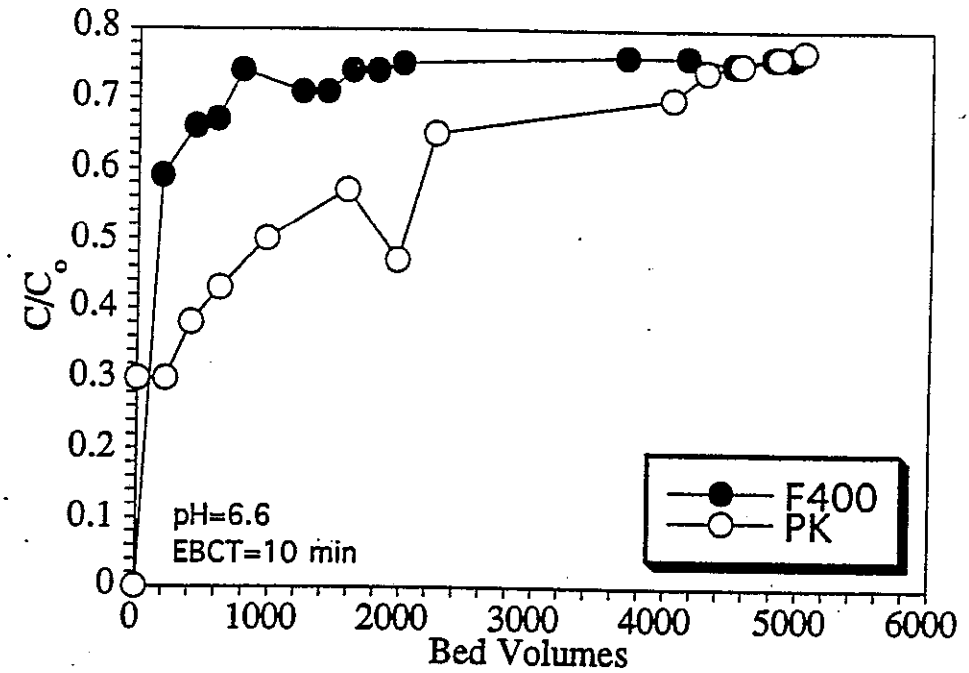

Figure 5.14. Effect of GAC on Bromate Reduction (SPW-II)

Table 5.6. Bed Volumes Required to Reach 50% Breakthrough

Source	EBCT	pH	F-400	F-300	PK
SPW	20	8.0	503	100	
SPW	5	8.0		2296	975
SPW	10	6.0	1000		
CCW	10	8.0	811		
CCW	10	6.0	1903		
CCW	4	6.8	400	–	–
ACW	10	8.0		450	
ACW	10	6.0			
ACW	5	8.0			
SLW	10	6.0	730	6000	
SLW	5	8.0			
LAW	10	6	377	1468	
LAW	10	7.8	250	900	200
MQW	10	6.0	1141	7000	–

Conclusions

Bromate removal by activated carbon was found to be a two step process: adsorption followed by chemical reduction. Bromate removal is dependent upon pH of the source water, type of activated carbon and the contact time. An inverse trend was observed between the concentration of metals on the surface of the carbon and the percentage removal of bromate. Bromate removal by RSSCT columns was more effective than bromate removal in batch experiments for the same contact time. Hence bromate removal using the normal PAC doses may not be feasible in a flocculation chamber. Bromate removal using RSSCT columns was significantly faster than in batch tests presumably due to higher diffusion capability.

These preliminary results indicate that an average of 30-40% bromate can be continuously removed atleast for two months in a continuous full-scale GAC column. Although the RSSCT results shows promise, some caution is needed in interpreting success so far. The results of RSSCT compare those of a very small pilot plant column which was fed in the lab with a single batch of water obtained from a water treatment plant and spiked with a known concentration of bromate. The pilot plant, therefore, cannot account for variations in water quality that would occur had the column been fed with plant water over a period of months. One of the strong points of the RSSCT is that it can be applied at different points and times throughout the year, allowing a lot of data to be gathered on raw water variations.

NOM fouling can reduce the adsorption capacity in pilot or full scale plants. However, a reduction in bromate removal capacity is not anticipated in an RSSCT column because breakthrough of NOM is completed before bromate breakthrough so that fouling cannot occur thus violating a basic assumption that equal adsorption capacities in both RSSCT and full scale tests is violated.

Recommendations

Predictive tools, like dynamic modeling or RSSCT, may be useful in deciding upon the design and operation of pilot plants. Regardless of future developments with modeling approaches, it is difficult to envision that utilities will accept these without some verification at the pilot plant scale; an investment of even a few hundred thousand dollars in such studied is still worthwhile considering the large investment anticipated in a GAC facility. Also pilot plants allow the impact of biodegradation to be measured and provide a way to measure GAC loading along the bed length.

Complete RSSCT data for various experiments is summarized in Tables 5.7 to 5.17.

Table 5.7. RSSCT Evaluation: SPW-I ($[BrO_3^-]_0$= 45 µg/L, EBCT=10 min)

Carbon	F-400 (pH=7.8)		F-300 (pH=7.8)		F-300(pH=6.0)	
Bed Volumes	$\frac{[DOC]}{[DOC]_0}$	$\frac{[BrO_3]}{[BrO_3]_0}$	$\frac{[DOC]}{[DOC]_0}$	$\frac{[BrO_3]}{[BrO_3]_0}$	$\frac{[DOC]}{[DOC]_0}$	$\frac{[BrO_3]}{[BrO_3]_0}$
10	0.06	0.01	0.06	0.01	0.06	0.01
50	0.03	–	0.06	0.24	0.06	0.09
100	0.14	0.44	0.1	0.58	0.09	0.09
188	0.21	0.59	0.1	0.83	0.09	0.11
396	0.21	0.64	0.12	0.75	0.11	0.15
550	0.12	0.67	0.13	0.82	0.10	0.25
850	0.18	0.75	0.2	0.79	0.19	0.29
1280	0.24	0.72	0.2	0.83	0.19	0.31
1630	0.26	0.74	0.23	0.85	0.20	0.38
1740	0.39	0.74	0.23	0.85	0.22	0.40
3820	0.35	0.76	0.43	0.81	0.41	0.59
4180	0.37	0.79	0.7	0.87	0.68	0.66
4590	0.37	0.79	0.83	0.88	0.80	0.70
4910	0.39	0.76	0.83	0.85	0.80	0.74

Table 5.8. RSSCT Evaluation: SPW-II (Amb.pH , F400, EBCT 20min)

Bed Volume	DOC mg/L	$\frac{[DOC]}{[DOC]_0}$	BrO_3^- ug/L	$\frac{[BrO_3^-]}{[BrO_3^-]_0}$
0	1.75	1.00	42	1.00
94	0.25	0.14	14	0.35
173	0.15	0.09	19	0.45
503	0.37	0.21	25	0.60
671	0.25	0.14	25	0.61
849	0.50	0.29	29	0.68
1627	0.37	0.21	29	0.68
1903	0.40	0.23	28	0.68
1997	0.31	0.18	29	0.69
2146	0.25	0.14	29	0.69
2359	0.20	0.12	30	0.71
2469	0.22	0.13	29	0.69
2830	0.35	0.20	34	0.81
4104	0.33	0.19	36	0.85
4403	0.39	0.22	38	0.90
4749	0.43	0.25	39	0.93

Table 5.9. RSSCT Evaluation: SPW (II) (Treated) (pH=6.0, PK, EBCT=10min)

Bed Volume	DOC mg/L	$\frac{[DOC]}{[DOC]_o}$	BrO_3^- ug/L	$\frac{[BrO_3^-]}{[BrO_3^-]_o}$
Initial	1.75	1.00	42	1.00
6.3	0.69	0.39	12	0.30
220	0.12	0.07	12	0.30
408	0.16	0.09	16	0.38
622	0.22	0.13	18	0.43
975	0.30	0.17	21	0.50
1579	0.40	0.23	24	0.57
1965	0.55	0.31	20	0.47
2249	0.58	0.33	27	0.65
4041	0.97	0.55	29	0.70
4293	1.06	0.61	31	0.75
4560	1.17	0.67	37	0.87
4844	1.18	0.67	32	0.76

Table 5.10. RSSCT Evaluation: CCW-I (pH=6.8, PK, EBCT 10min)

Bed Volume	DOC mg/L	$\frac{[DOC]}{[DOC]_o}$	BrO_3^- ug/L	Bromide ug/L	$\frac{[BrO_3^-]}{[BrO_3^-]_o}$
Initial	1.721	1.00	66	152	1.00
94	0.234	0.14	11	54	0.17
188	<0.1	0	38	138	0.58
283	<0.1	0	44	154	0.66
519	<0.1	0	47	164	0.72
676	<0.1	0	48	164	0.74
849	<0.1	0	49	155	0.74
1038	<0.1	0	49	156	0.74
1368	<0.1	0	49	176	0.74
1745	<0.1	0	50	155	0.75
2264	<0.1	0	50	170	0.75
4718	1.193	0.69	58	175	0.88
4954	1.218	0.71	50	167	0.76
5142	1.342	0.78	58	177	0.88
5850	1.147	0.67	53	n/a	0.80

Table 5.11. RSSCT Evaluation: CCSW-I (Treated) (pH=6.8, F400, EBCT=10min)

Bed Volume	DOC mg/L	$\frac{[DOC]}{[DOC]o}$	BrO_3^- ug/L	Bromide ug/L	$\frac{[BrO_3^-]}{[BrO_3^-]_0}$
Initial	1.6	1	67	88	1.00
188	0.2	0.13	26	0	0.39
377	0.4	0.25	25	0	0.37
566	0.5	0.31	31	0	0.47
754	0.55	0.34	37	0	0.55
1132	0.6	0.37	40	65	0.60
1509	0.66	0.41	42	0	0.63
1887	0.56	0.35	46	79	0.69
3459	0.55	0.34	51	94	0.76
3836	1.1	0.69	54	69	0.80
4214	1.2	0.75	55	93	0.82
4591	1.2	0.75	55	93	0.82

Table 5.12. RSSCT Evaluation: CCSW-I (Treated) (pH=6.8, F400, EBCT=4min)

Bed Volume	DOC mg/L	$\frac{[DOC]}{[DOC]o}$	BrO_3^- ug/L	Bromide ug/L	$\frac{[BrO_3^-]}{[BrO_3^-]_0}$
Initial	1.60	1.00	65	88	1.00
591	0.90	0.56	53	72	0.82
887	0.94	0.59	51	73	0.78
1330	1.00	0.63	52	86	0.79
1774	1.25	0.78	57	91	0.87
2217	1.31	0.82	55	93	0.84
2661	1.30	0.81	56	93	0.85
3568	1.28	0.80	56	90	0.85
4656	1.25	0.78	56	97	0.86

Table 5.13. RSSCT Evaluation: CCSW-II (Treated) (pH=6.8, F400, EBCT 10min)

Bed Volume	DOC mg/L	$\frac{[DOC]}{[DOC]_o}$	BrO_3^- ug/L	$\frac{[BrO_3^-]}{[BrO_3^-]_o}$
Initial	1.71	1.00	44	1.00
188	0.54	0.32	27	0.63
377	0.12	0.07	25	0.58
591	0.17	0.10	24	0.55
811	0.18	0.11	37	0.84
1289	0	0	40	0.91
1824	0.29	0.17	38	0.86
2374	0.37	0.22	38	0.86
4529	0.58	0.34	38	0.88
4894	0.63	0.37	38	0.88
5315	0.86	0.50	38	0.88
5573	0.83	0.49	38	0.88
6029	0.90	0.53	38	0.88
6369	0.94	0.55	38	0.88
6778	1.08	0.63	38	0.88
7209	1.15	0.67	38	0.88

Table 5.14. RSSCT Evaluation: CCSW-II (Treated) (pH=6.0, F400, EBCT=10min)

Bed Volume	DOC mg/L	$\frac{[DOC]}{[DOC]_o}$	BrO_3^- ug/L	$\frac{[BrO_3^-]}{[BrO_3^-]_o}$
Initial	1.71	1.00	60	1.00
94	1.04	0.61	10	0.18
173	0.10	0.06	20	0.34
503	0.38	0.22	25	0.42
671	0.38	0.22	27	0.46
849	0.16	0.09	27	0.46
1627	0.36	0.21	30	0.50
1903	0.34	0.20	31	0.52
1997	0.47	0.27	38	0.63
2146	0.53	0.31	40	0.67
2359	0.56	0.33	41	0.70
2469	0.55	0.32	42	0.71
2830	0.71	0.42	43	0.73
4104	0.80	0.47	44	0.75

Table 5.15. RSSCT Evaluation: LAW (Treated) (pH=7.8, PK, EBCT=10min)

Bed Volume	DOC mg/L	$\frac{[DOC]}{[DOC]_o}$	BrO_3^- ug/L	$\frac{[BrO_3^-]}{[BrO_3^-]_o}$
Initial	2.43	1.00	53	1.00
188	0.62	0.26	38	0.72
566	0.53	0.22	41	0.78
1022	0.59	0.24	42	0.80
1400	0.88	0.36	44	0.83
1588	0.91	0.37	45	0.84
1777	0.96	0.40	40	0.75
1966	1.07	0.44	39	0.73
3664	1.13	0.47	46	0.88
4120	1.51	0.62	38	0.72
4309	1.69	0.70	35	0.66
4498	1.62	0.67	35	0.67
4686	1.59	0.65	35	0.66
5001	1.66	0.68	35	0.67

Table 5.16. RSSCT Evaluation: LAW (Treated) (EBCT=10 min, BrO_3^-=40 µg/L)

Carbon	F-300 (pH=6.0)		F-400 (pH=7.8)		F-400(pH=6.0)	
Bed Volumes	$\frac{[UV]}{[UV]_o}$	$\frac{[BrO_3]}{[BrO_3]_o}$	$\frac{[DOC]}{[DOC]_o}$	$\frac{[BrO_3]}{[BrO_3]_o}$	$\frac{[DOC]}{[DOC]_o}$	$\frac{[BrO_3]}{[BrO_3]_o}$
10	0.02	0.01	0.02	0.05	0.02	0.03
35	0.02	0.17	0.04	0.15	0.05	0.16
104	0.03	0.17	0.09	0.25	0.08	0.22
220	0.03	0.25	0.21	0.45	0.12	0.35
460	0.03	0.36	0.19	0.69	0.15	0.48
745	0.04	0.45	0.22	0.70	0.20	0.53
1468	0.04	0.60	0.25	0.72	0.25	0.66
3708	0.09	0.72	0.46	0.75	0.39	0.74
3862	0.09	0.72	0.49	0.76	0.40	0.75
4262	0.09	0.78	0.53	0.84	0.45	0.78
4450	0.11	0.77	0.54	0.85	0.45	0.79
4733	0.23	0.78	0.53	0.83	0.46	0.82

Table 5.17. RSSCT Evaluation: ACW (Treated)
F300, $(BrO_3^-)_{raw}$=66 µg/l, $(UV)_{raw}$=0.179

Bed Volumes	$\frac{[UV]}{[UV]_0}$	Br^- ug/L	$\frac{[BrO_3^-]}{[BrO_3^-]_0}$
26	0.145	48	0.18
145	0.173	146	0.44
368	0.307	157	0.67
569	0.379	165	0.71
1102	0.541	172	0.79
1586	0.587	169	0.79
2181	0.604	159	0.83
5160	0.782	161	0.91
6054	0.782	162	0.86
6501	0.785	165	0.88

Part VI

Bromate Destruction Using UV Irradiation (After Pre-ozonation or Intermediate Ozonation)

Recognizing that activated carbon may not be cost-effective for all utilities, the use of ultraviolet irradiation for BrO_3^- destruction has been evaluated. UV irradiation can be used for disinfection although it is not considered cost-effective; however, it may be more viable if it also achieves BrO_3^- removal and other DBP destruction. Bromate destruction initially in raw source waters was compared with treated source waters. Since bromate destruction was better in treated waters, all subsequent experiments were performed in treated source waters.

Chemistry. The destruction of bromate can be represented as follows with the formation of hypobromite ion as an intermediate.

$$BrO_3^- \xrightarrow{uv} OBr^- + O_2$$
$$OBr^- \xrightarrow{uv} Br^- + 1/2\ O_2 \qquad \text{----(6.1)}$$

UV irradiation in the wavelength range of 180-300 nm provides energy ample for producing intermolecular changes of the bromate molecules. The decomposition of bromate leads to the production of bromide and oxygen as end products via complex reactions which are initiated by the products generated by the primary reactions of photolysis. The reaction proceeds through internal transition of bromate and does not involve a charge-transfer-to-solvent (CTTS) intermolecular process (Amichai et al., 1969).

UV light is part of the electromagnetic spectrum between visible and X-rays. The portion of the UV spectrum between 190-220 nm is considered effective with a peak effectiveness of around 195 nm for bromate destruction.

Kinetics. The equation for bromate destruction in which UV intensity (î in $\mu W/cm^2$) can be considered everywhere uniform is given by:

$$\frac{[BrO_3^-]}{[BrO_3^-]_o} = e^{-k\hat{i}\theta} \qquad \text{-----(6.2)}$$

where $\theta=V/Q$ [V=Volume of reactor, gal; Q =water flow rate, gpm] is irradiation contact time (sec) and k = rate constant of bromate destruction ($cm^2/\mu w$-sec).

The UV dose ($\mu W/cm^2$) required for bromate destruction is a function of the lamp's UV intensity multiplied by the exposure time. The UV dose required for satisfactory destruction of bromate can be calculated according to the initial bromate concentration (and also depends upon background water characteristics related to UV absorbing material). Different waters exhibit different type of organic matter, alkalinity, and nitrate ion and hence may exhibit different UV absorbance properties.

Low Pressure vs Medium Pressure Lamp. A commonly used UV source for water wastewater treatment is the low pressure mercury vapor lamp. The spectral output of this lamp is mostly at the 254 nm position with some output at 185 nm which is often absorbed by poor quality quartz used as the envelop of the lamp. This line can be used if the quartz in the lamp is replaced with high quality quartz (such as Suprasil) which is transparent to 185 nm radiation. Medium pressure mercury lamps operating in the "medium" or "high" pressure range, with or without dopants to affect the distribution of wavelenths emitted. With an input power of 15-80 watts, the UV frequency emitted is ≈254 nm in the germicidal range and 185 nm in the shorter wave length range. UV intensity can be varied by increasing the number of lamps, changing voltage, or by employing a medium pressure lamp. Emitting a high output in the 200-300 nm range, a single medium pressure tube can replace up to 50 low pressure arc-tubes. In addition, the medium pressure lamps are unaffected by fluid temperature. The energy required for destruction of various microorganisms has been compared with bromate as shown in Table 6.1.

Table 6.1. UV Energy Required for Destruction of Various Microorganisms and Bromate (μW-sec/cm^2) at 254 nm.

Application	Bacteria	Protozoa	Viruses	Bromate
Energy Required	9000-27000	22,000-200,000	7,000-9,000	30,000-50,000
Reference	Aquafine, 1988	Aquafine, 1988	Aquafine, 1988	This study

Experimental Matrix. The experimental matrix and ranges of variables studied for bromate destruction by UV irradiation in different source waters is summarized in Table 6.2

Table 6.2. Experimental Matrix for Bromate Reduction By UV Irradiation Experiments

Source	Instrument A			Intrument B			Instrument C			Instrument D		
	5 min	10 min*	15 min	5 min	10 min	15 min	30 sec	60 sec	120 sec	4 sec	20 sec	30 sec
CRW	√	√	√	√	√	√	–	–	–	–	–	–
SPW	√	√	√	√	√	√	√	√	–	√	√	√
CCW	√	√	√	√	√	√	–	–	–	–	–	–
ACW	√	√	√	√	√	√	–	–	–	–	–	–
LAW	√	√	√	√	√	√	–	–	–	–	–	–
SLW	√	√	√	√	√	√	√	√	√	√	√	√
MQW	√	√	√	√	√	√	√	√	√	√	√	√

* experiments were performed at three different pH levels

Batch Experiments (Intruments A and B)

The photo decomposition of BrO_3^- leads to the production of Br^- and oxygen as end products, and of bromine ($\sum[BrO^-+HOBr]=HOBr_t$) as an intermediate. The concentration changes of these three species during a typical UV irradiation run is shown in Figure 6.1 (Instrument B, Quartz Q2).

Effect of pH. pH had no significant effect on BrO_3^- reduction by UV irradiation in the pH range tested (pK_a of $HBrO_3$ is very low ≈ 2). This also shows that production of free radicals during UV irradiation has no significant effect on bromate reduction unless strong reducing agents such as aqueous free electrons (e^-_{aq}) and hydrogen atoms (H·) are produced.

Effect of contact time. Much higher contact times were required to reduce bromate using the traditional UV disinfection units (A, B) ostensibly due to the majority of radiation being emitted at 254 nm (Table 6.3). Normal contact times employed during disinfection using these UV units range from 15-25 secs which are relatively much lower than needed to reduce bromate. In other words, the use of these UV disinfection units for bromate destruction is not economically feasible and realistic.

Effect of DOC. The presence of organic matter (DOC) lowered the reduction of BrO_3^- and decreased the production of Br^- in natural waters, due to presumably some absorption of UV energy and the consumption of free radical species by organic carbon (Figure 6.2*; Instrument B). The presence of bromine can lead to the formation of organic bromine because of secondary reactions between humic material and bromine in the irradiated solutions of BrO_3^-. Upon UV irradiation of distilled water containing high levels of Br^-, no BrO_3^- was formed indicating that UV irradiation can be used irreversibly to convert BrO_3^- to Br^-.

Effect of Source Water. A range of source waters from low TDS to high TDS concentration (alkalinity ranging from 20-120 mg/L $CaCO_3$) were investigated and the general trend was better removal in low TDS/low DOC/low alkalinity waters. High TDS source waters contain ions like carbonate, nitrate and other UV absorbing ions which may hinder UV absorbance and decomposition of bromate.

---

* Equation 6.2 was used to evaluate k_1'

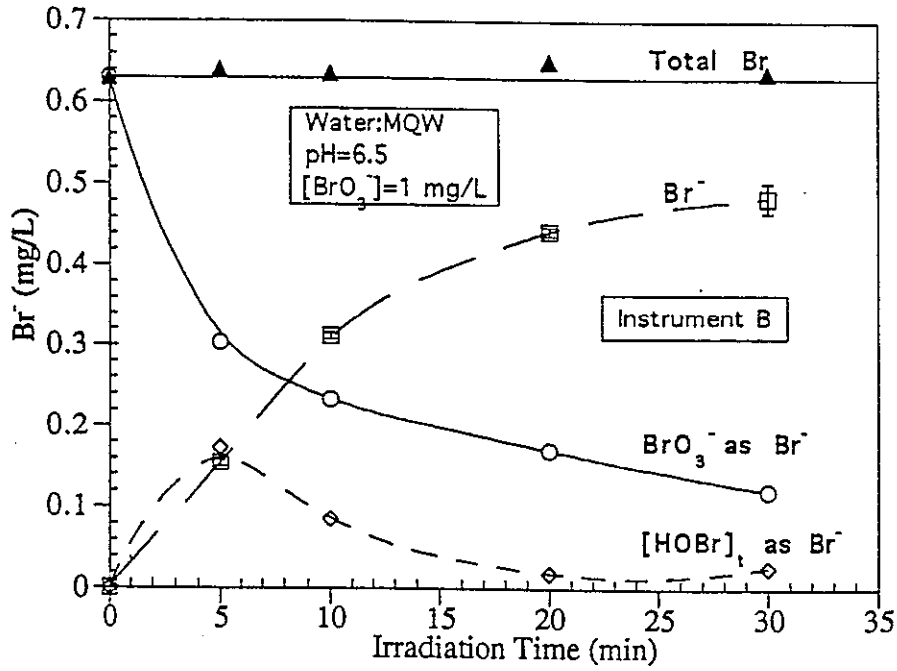

Figure 6.1. UV Irradiation of BrO_3^- Solution: Formation of HOBr/OBr^- and Br^-

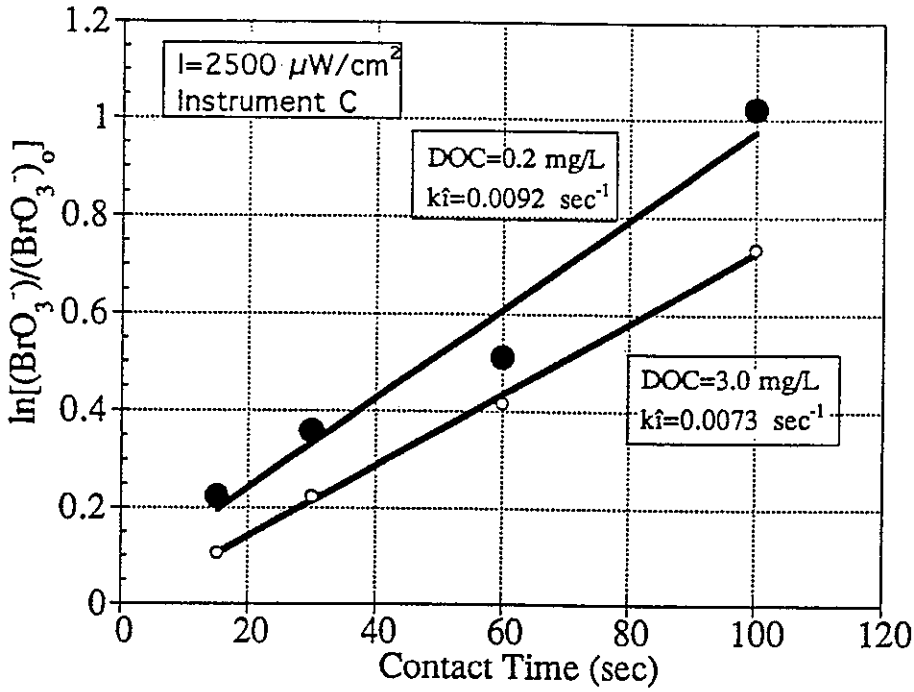

Figure 6.2. Effect of DOC on Bromate Removal

Table 6.3. Bromate Reduction Using Instruments A and B*

Source	BrO_3^-	Contact Time	% Reduction (Instrument A)	% Reduction (Instrument B)
---	µg/L	min	---	---
CRW	25	5	25	30
CRW	25	10	38	40
CRW	50	5	20	28
SPW	25	5	20	25
SPW	25	10	36	41
SPW	50	5	24	32
CCW	25	5	22	30
CCW	50	5	25	25
ACW	25	5	36	42
ACW	25	10	41	44
ACW	50	5	34	38
SLW	25	5	36	37
SLW	25	10	46	45
SLW	50	5	35	40
MQW	25	5	38	44
MQW	50	5	32	40

* all of source waters shown in this Table were treated source waters

The quartz tube Q2 used in instrument B allowed upto 6% of radiations in the range of 180-200 nm; presumably because of this bromate destruction was found to be relatively better than instrument A for the same exposure levels.

The results of experiments conducted using instruments A and B along with percentage bromate reduction UV exposure times are shown in Table 6.3.

Continuous Flow Experiments (Instrument C)

Instrument C was found to be better than instruments A and B for bromate destruction and this instrument allowed higher radiations in 180-200 range than instruments A and B.

Effect of Flow Rate. Flow rates ranging from 7 to 48 ml/min with contact times equal to 15 - 120 secs were evaluated and the results are summarized in Table 6.4.

Effect of UV Intensity. The effect of varying UV intensity on bromate destruction was evaluated and the results are shown in Figures 6.3 and 6.4 (Quartz Q3). On increasing the intensity from 850 to 2500 $\mu W/cm^2$ and maintaining a constant UV irradiation contact time, bromate destruction efficiency increased from 3% to more than 50% with an initial bromate concentration of 50-100 $\mu g/L$.

Effect of quartz type. The effect of two different quartz types (Quartz Q3 and Quartz Q3C) on bromate destruction was evaluated. The percentage transmittance curves for these quartz tubes are given in Figure 6.5. The quartz sleeve Q3 which emits most of radiations in the <200 nm range was more effective than the other quartz tube presumably due to better absorption of UV by bromate molecules in that range (equation 1, Figure 6.6). UV radiation light in the range of 170-200 nm is relatively energetic (70-471 kJ/mole) and is more efficient in breaking molecular bonds than higher wavelength light. For example, UV light < 180 nm is responsible for the photolysis of chloroflorocarbons (CFCs) in the stratosphere and can cleeve oxygen and water. Moreover, many compounds have much higher molar absorptivities at lower wavelengths (e.g., for CCL_4 ε_{254}=0.2, ε_{200}=170 and ε_{200}=2000 M^{-1} cm^{-1}). Quartz Q3C unlike most other synthetic fused quartz materials has a very low hydroxyl content (< 10 ppm) and the high purity of this material allows maximum transmittance of UV radiation. The virtual absence of bulk metallic impurities in quartz Q3C greatly reduces the solarization rate of fused quartz and therefore minimizes the time dependent darkening effect which is often seen in irradiated natural quartz. Also purity of quartz Q3C also means longer useful lifetimes. Although quartz Q3C produced upto 0.6 mg/L of

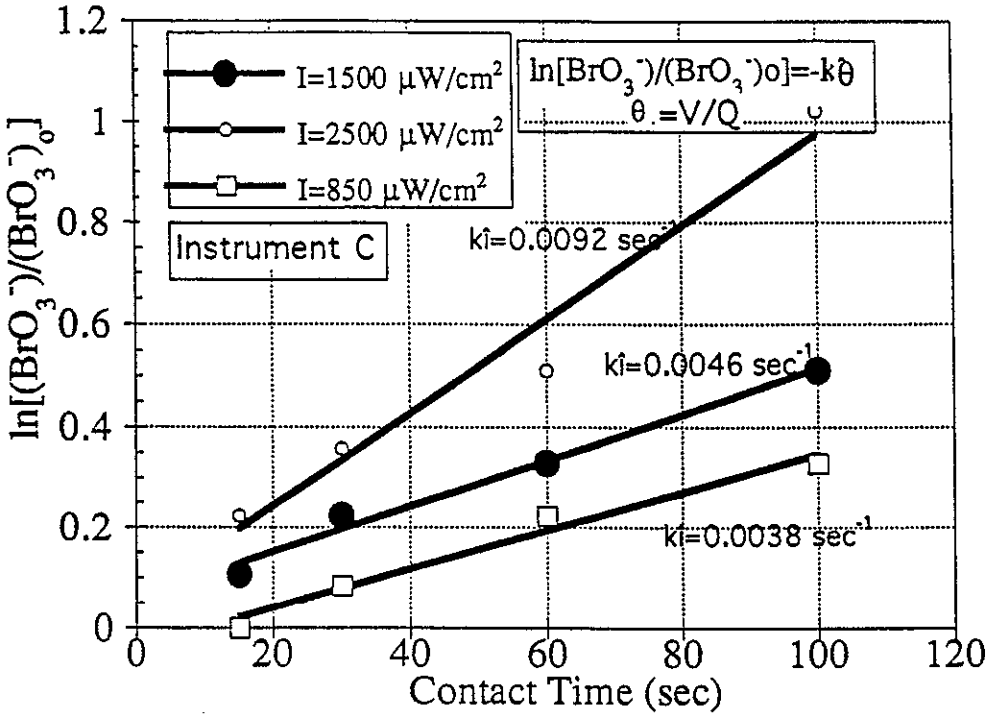

Figurte 6.3. Effect of UV Intensity on Bromate Reduction

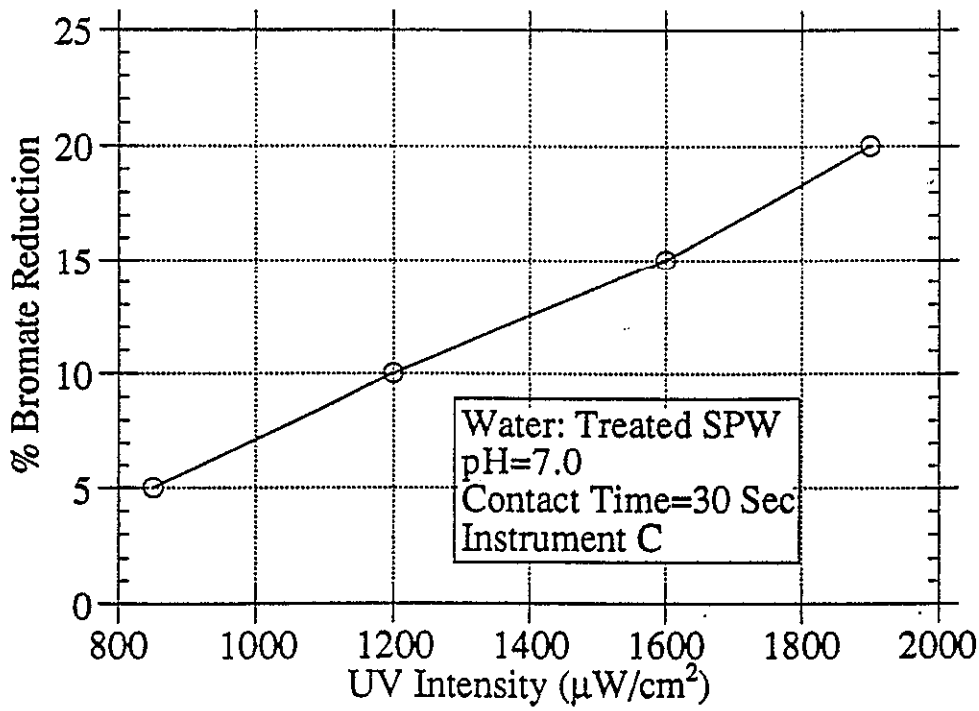

Figure 6.4. Effect of UV Intensity on Bromate Reduction

Table 6.4. Bromate Destruction Using Low-Pressure UV Lamp in MQW

Sample	BrO_3^- ug/L	Intensity uW/cm^2	Flow Rate ml/min	Contact Time sec	% BrO_3^- Reduction	% Bromide Unaccounted
1	50	control	33	27	0	0
2	50	850	33	27	3	100
3	50	1200	33	27	7	70
4	50	1600	33	27	13	60
5	50	1200	16	54	18	40
6	50	1900	48	15	9	65
7	50	1900	24	30	19	30
8	50	1900	11	80	29	20
9	50	1900	7	120	38	20

Table 6.5. Bromate Destruction Using Medium Pressure Mercury Lamp

Sample	Water	BrO_3^- ug/L	Flow Rate ml/min	Contact Time sec	% BrO_3^- Reduction
1	MQW	50	1 GPM	30	100
2	MQW	100	1 GPM	30	100
3	MQW	50	1.5 GPM	20	78
5	MQW	50	8 GPM	4	75
6	MQW	100	8 GPM	4	65
7	KCW*	50	1 GPM	30	100
8	KCW	100	1 GPM	30	87
9	KCW	100	1.5 GPM	20	86
11	KCW	50	8 GPM	4	46
12	KCW	100	8 GPM	4	45

* City Water from Kenton County Water District, KY (DOC≈1.5 mg/L)

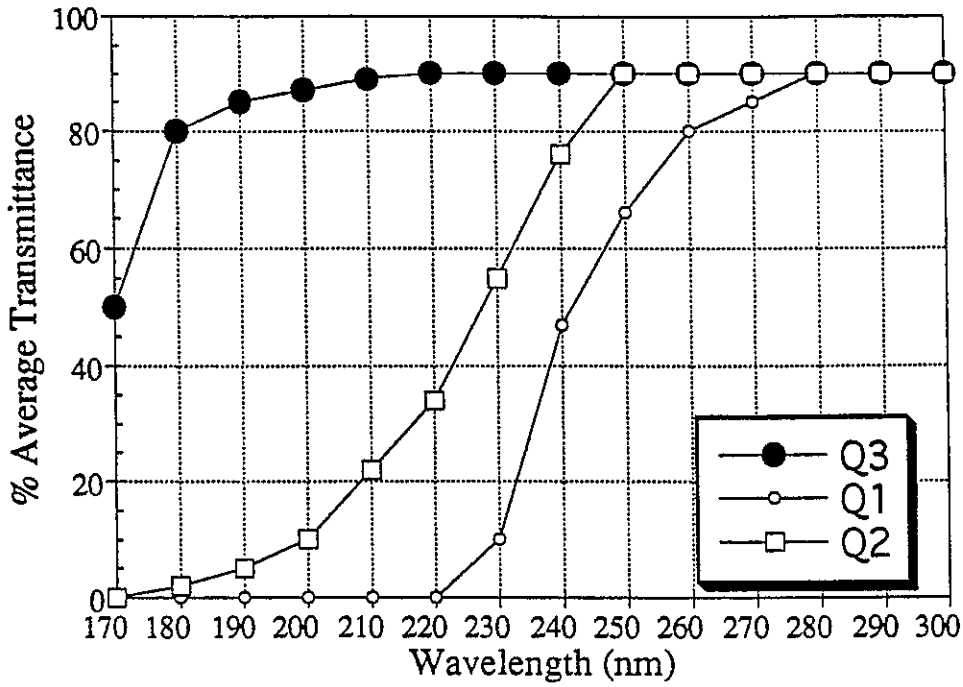

Figure 6.5. Quartz Type vs Transmittance of Radiations at Different Wavelengths

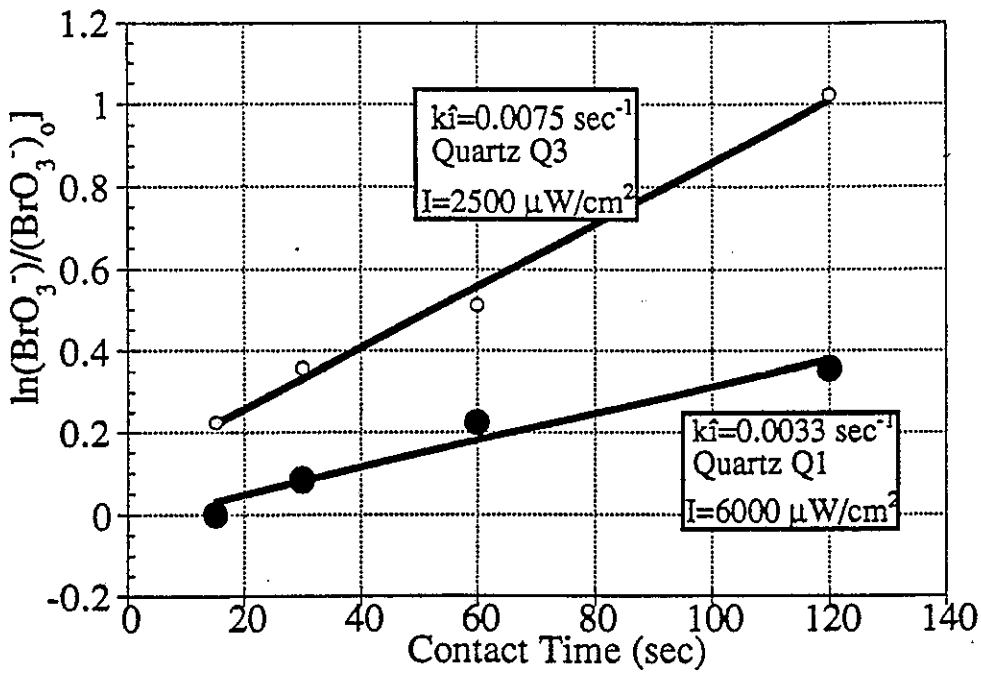

Figure 6.6. Effect of Quartz Tube on Bromate Reduction

ozone in the gas phase for the contact times employed in this study, no conversion of bromide ion to bromate ion was found (0.6 mg/L ozone in gas phase translates into less than 0.1 mg/L residual ozone in source waters containing DOC in the 3-4 mg/L range) but an added advantage of additional disinfection without producing ozone biodegradable by-products since all higher molecular weight DOC fractions are presumed to have been removed at this stage.

Table 6.4 shows the effect of UV dose on bromate destruction and the amount of bromide recovered (quartz Q3). Because of low concentrations of bromate conversion to bromide, none of the bromide in bromate disappeared was accounted for (Br^- detection limit $\approx$ 10 µg/L). The percentage of unaccounted bromide decreased as the percentage of bromate destruction increased.

Continuous Flow Experiments (Instrument D)

To compare bromate destruction with a low pressure mercury lamp, a medium pressure mercury lamp with an intensity of 500 mW/cm^2 was evaluated (design flow rate of 25 gpm). This intensity is much higher than instruments A, B and C. The energy distribution of the medium pressure arc-tube employed in this research is shown in Figure 6.7 and compared with a low pressure lamp. The energy distribution in a medium pressure lamp varies from a broad range of 180 to 360 nm in contrast to most of radiation emitted at 254 nm in a low pressure lamp. Medium pressure lamps are now avilable with various dopants added that enhance emissions below 250 nm. These are avilable in the range of 20-40 kW.

Effect of contact time. Contact times of as low as 10 sec resulted in almost complete destruction of bromate with an initial bromate concentration of 50-100 ug/L (Table 6.5). At a flow rate of about 8 gpm, the UV dose was about 600 mW-sec/cm^2 and, for dose rates higher than these, putting two UV chambers in series would be feasible.

Effect of source water. Two source waters (MQW and KCY) were evaluated and percentage reductions of bromate ranged from 65-90% in KCW (DOC=1.5 mg/L) and from 70-100% in MQW (DOC=0.2 mg/L) for contact times ranging from 4 to 30 secs. pH (6-8) and temperature (15-25 °C) had no effect on bromate reduction.

Conclusions and Recommendations

As with other bromate removal processes, bromate was found to be reduced to bromide ion indicating that bromate removal by all these processes is an irreversible phenomenon. UV irradiation to remove bromate using low pressure

mercury lamps was not effective and very high contact times were necessary to reduce bromate under normal circumstances used for disinfection. However, employing a quartz sleeve which allowed most of UV radiations in the 180-200 nm range was more effective. A medium pressure mercury lamp was highly effective for contact times as low as 5 secs to reduce bromate by more than 80% with an initial concentration of 50 μg/L. Addition of ammonia at various concentrations had virtually no effect on the efficiency of bromate reduction for the bromate range normally encountered during drinking water treatment. pH had no effect on the UV irradiation of water containing bromate ion indicating UV process is effective at all pH levels contrary to other bromate removal processes. Temperature and pH had no effect on bromate reduction using a medium pressure lamp.

Since oxygen strongly absorbs from 120-200 nm, forming oxygen atoms and subsequently ozone, a UV lamp reactor operating in this range should also produce a variety of free radicals which can decompose bromate to bromide ion. Also since the absorption coefficient of H_2O at 185 nm is also high and the quantum yield for decomposition to hydrogen atoms (H·) and OH radicals is respectable (0.3). H atoms are reducing agents and will help reduce bromate ion to bromide ion.

Part VII

Conclusions and Recommendations

Several methods have shown promise in removing BrO_3^- applicable to conventional surface treatment plants contemplating the use of ozone at various points of application. The main conclusions from this project are:

(1) In all processes evaluated, Br^- was found after treatment ($\geq$ 90% recovery of influent Br associated with BrO_3^-), indicating that chemical reduction (aqueous or surface) is dominating as opposed to adsorption (to floc or activated carbon). BrO_3^- is reduced to Br^- during the treatments discussed in this paper; thus, Br^- may still play a role in the formation of brominated DBPs during post-chlorination.

(2) The presence of background DOC had a significant effect on BrO_3^- reduction using Fe^{2+}, GAC, and UV irradiation. pH variation had a strong effect on BrO_3^- reduction using Fe^{2+} and activated carbon but had a insignificant effect on UV irradiation. Removal of BrO_3^- with PAC averaged 0.02-0.45 mg BrO_3^-/g carbon based on batch experiments and the type of PAC. The results obtained in this study using PAC indicate that the rate determining step for the removal of bromate is apparently the rate of diffusion of bromate through the laminar layer surrounding the surface of the activated carbon. The rates of bromate removal by most PACs are dependent upon the carbon particle size, the initial bromate concentration, the ionic species in water, and the temperature. The effect of anion species (e.g., sulfate) on the removal of bromate by PACs is quite interesting and is indicative of anion exchange and reduction rather than adsorption.

(3) Chemical reduction of BrO_3^- to Br^- is feasible through the use of ferrous iron (Fe^{2+}) as a reducing agent which itself is then converted to ferric iron (Fe^{3+}). In reacting with BrO_3^- and the dissolved oxygen present in an ozonated water, Fe(II) is oxidized to Fe(III) which can then function as a coagulant for DBP precursors. The ferrous reduction studies were performed primarily in water with ambient dissolved oxygen (DO) levels. However, after ozonation, DO could be as high as 15-20 mg/L. Future work is needed to evaluate the effect of higher DO.

(4) Use of GAC (RSSCT) columns showed almost complete removal of BrO_3^- followed by gradual breakthrough. BrO_3^- breakthrough was much slower than DOC breakthrough (SLW) indicating that GAC columns can be used emplyed

to remove BrO_3^- in low DOC waters and chemically pretreated waters, and for much longer times than for DOC removal. BrO_3^- removal capacities were found to be dependent on source water characteristics and initial BrO_3^- concentration. Removal of BrO_3^- with GAC averaged 0.79mg BrO_3^-/g carbon based on RSSCT-GAC experiments for SPW (pH=8.0, DOC=3.7 mg/L) and 3.42 mg BrO_3^-/g carbon for SLW (50% breakthrough, pH=7.0, DOC=3 mg/L).

(5) UV besides providing disinfection, irradiation can also reduce BrO_3^- but its cost of operation has not been adequately evaluated for this purpose. Bromate destruction by UV irradiation using both low pressure mercury lamp amd medium pressure mercury lamp has been evaluated. Bromate was shown to be reduced to bromide ion with bromine as an intermediate for a contact time ranging from 15 secs to 2 minutes. Bromate destruction using low pressure mercury lamp ranged from 10 to 50 % for contact times and conditions normally employed for disinfection (I=2000 - 6000 $\mu W/cm^2$). Almost complete destruction was achieved using a medium pressure mercury lamp with an initial bromate concentration of 50 $\mu g/L$(dose=30 mW/cm^2) and contact time of 4-30 sec.

The advantages of UV lamps emitting in the low wavelength range are not well appreciated or exploited by the water supply industry. Further research and technology transfer is needed to evaluate the efficiencies, costs, and reliability factors for UV lamps. UV lamp manufacturerers have a great deal of technology that has been developed for industrial applications that might be transferred to water treatment uses.

The effectiveness of various methods for removing bromate from drinking water is summarized in Table 7.1.

Table 7.1 Summary of Bromate Various Removal Methods and Their Effetiveness

Technique	Conditions	Effectiveness and Benefits	Capital Cost
Ferrous Reduction	• DO ≤ 10 mg/L • pH < 8.0	• 30-50% Reduction • Works as coagulant	Low
PAC (Flocculator)	• Contact Time ≈ 20-40 min • Dose= 25-50 mg/L • PAC Specific	• 10-30% Reduction • Removes DOC • Removes SOCs	Moderate
GAC Column	• Low TDS • Low DOC Treated Water • GAC Specific	• 50-100% Removal • Removes DOC • Removes SOCs	Moderate
Ion Exchange Resins	• Low chloride and sulfate • Low DOC treated water	• 100% Removal • Removes Aresenic	Moderate
UV Irradiation	• Low DOC, low alkalinity • Contact time<10 sec (Medium pressure lamp) • Contact time>30 sec (Low pressure lamp)	• 10-100 % • No pH effect • Ease of maintenance • Added disinfection	Low
Electron Beam Irradiation	• 50-100 krads • Contact time ≤ 20 sec	• 50-100% Removal • TOC removal • Destroys other DBPs	High

Part VIII

References

(1) Amichai, O, G. Czapski, and A. Treinin, "Flash Photolysis of the Oxybromine Anions", *Israel J. Chem.*, 7:351-359, 1969.

(2) Amy, G., M. Siddiqui, K. Ozekin, and P. Westerhoff, "Threshold Levels for Bromate Formation in Drinking Water", Proceedings IWSA Workshop, Paris, 169-180, 1993a.

(3) Amy, G., M. Siddiqui, W. Zhai, and J. Debroux, "Nationwide Survey of Bromide in Drinking Waters", Final Report Submitted to AWWARF, 1994.

(4) Buxton, G., Greenstock, C., Helman, W., Ross, A., J. Phys. Chem. Ref. Data., 17:2, 677, 1988.

(5) Chapin, R.M. "The Effect of Hydrogen-ion Concentration on the Decomposition of Hypohalites," J. Am. Chem. Soc., 56:2211, 1934.

(6) Crecelius, E.A. "The Production of Bromine and Bromate in Seawater by Ozonation," Ozonews 5:1-2, 1977.

(7) Daniel, P. A., M. A. Zafer, and P. F. Meyerhofer, "Bromate Control: Water Quality, Engineering and Operational Considerations", 181-188, IWSA Workshop, Paris, 1993.

(8) Dougan W. K. and A. L. Wilson, "Absorptiometric Determination of Iron with T.P.T.Z"., *Water Treatment and Examination,* 22 , 1973.

(9) Galal-Gorchev, H. and J. C. Morris, "Formation and Stability of Bromamine, Bromimide, and Nitrogen Tribromide in Aqueous Solution", J. Inorg. Chem., 4:6:899, 1965.

(10) Glaze, W. H., H. S. Weinberg, and J. E. Cavanagh, "Evaluating the Formation of brominated DBPs During Ozonation", Journal AWWA, 85:1, 96-103, 1993.

(11) Gordon, G., "The Chemical Aspects of Bromate ion Control In Ozonated Drinking Water Containing Bromide Ion", 41-49, IWSA Workshop, Paris, 1993.

(15) Gramith, J. T., B.M. Coffey, S.W. Krasner, C. Kuo, E. G. Means, "Demonstration-Scale Evaluation of Bromate Formation and Control Strategies", AWWA Annual Conference, San Antonio, Texas, 1993.

(12) Haag, W.R and Hoigne, J., "Ozonation of Bromide-Contaning Waters: Kinetics of Formation of Hypobromous Acid and Bromate", Environ. Sci. Tech 17:261, 1983.

(13) Haag, W., and Hoigne, J., "Ozonation of Bromide-Containing Waters: Kinetics of Formation of Hypobromous Acid and Bromine in Water", Ozone Science & Engineering, 6:103, 1983.

(14) Haag, W., et al., "Improved Oxidation of Ammonia by Ozone in the Presence of Bromide Ion During Water Treatment", Water Research, 18:1125, 1984a.

(15) Hautman, D.P. and M. Bolyard, "Using Ion Chromatography to Analyze Inorganic Disinfection By-Products", Journal AWWA, 85:10, 88-93, 1993.

(16) Haruta, K., and T. Takeyama, "Kinetics of Reactions of Ozone with Inorganic Compounds and Disinfectants in Water", J. Phys. Chem., 85:2383-2388, 1981.

(17) Hoigne, J & Bader, H.,"The Role of Hydroxyl Radical Reactions in Ozonation Processes in Aqueous Solutions". Water Research, 10:377, 1976.

(18) Hoigne, J., and H. Bader, "Ozonation of Water:Oxidation-Competition Values of Different Types of Waters Used in Switzerland", Ozone: Science & Engineering, 1:357-372, 1979.

(19) Hoigne, J. "Mechanisms, Rates and Selectivities of Oxidants of Organic Compounds Initiated by Ozonation of Water." in Handbook of Ozone Technology and Applications, R. G. Rice and A. Netzer, Editors, Ann Arbor Science Publishers Inc, 341-379, 1982.

(20) Hoigne, J., H. Bader, W.R. Haag, J. Staehelin, "Rate Constants of Reactions of Ozone with Organic and Inorganic Compounds in Water-III", Water Research, 19:993-1004, 1985.

(21) Hoigne, J., H. Bader, and L. Howell, "Rate Constants For OH Radical Scavenging By Humic Substances: Role in Ozonation and In a Few Photochemical Processes for the Elimination of Micropollutants", Proceedings, ACS, Division of Environmental Chemistry, Denver, CO, April 1987.

(22) vander der J. H., Th. H. M. Noij and P.C.A. Ooms, "Analysis and Identification of Bromate in Water by Ion Chromatography and Multiple Detection at the Low-ppb Level", 25-32, IWSA Workshop, Paris, 1993.

(23) Krasner, S.W. et al., "The Occurence of Disinfection By-Products in US Drinking Water" Journal. AWWA, V.81, NO. 8, 1989.

(24) Krasner, S. W., Jill T. Gramith, and Edward G. Means, "Formation and Control of Brominated Ozone By-Products", Proceedings, Annual AWWA conference, Philadelphia, PA, 1991.

(25) Krasner, S. W., J. T. Gramith, B. M. Coffey, R. S. Yates, "Impact of Water Quality and Operational Parameters on the Formation and Control of Bromate During Ozonation", 157-168, IWSA Workshop, Paris, 1993.

(26) Krasner, S. W.,W. H. Glaze, H.S. Weinberg, P. A. Daniel, and I. Najm, "Formation and Control of Bromate During Ozonation of Waters Containing Bromide", Journal AWWA, 85:1, 73-81, 1993a.

(27) Kruithof, J. C. and R. T. Meijers, "Presence and Formation of Bromate in Dutch Drinking Water Treatment", 125-133, IWSA Workshop, Paris, 1993.

(28) Kuo, C, S.W. Krasner, G. A. Stalker, and H. S. Weinberg, "Analysis of Inorganic Disinfection By-products in Ozonation Drinking Water By Ion Chromatography", AWWA WQTC proceedings, San Diego, CA, 1990.

(29) Legube, B, B. K. Koudjonou, J.P. Croue, N. Merlet, "Influence of the Presence of NOM on Bromate Formation By Ozonation", 57-67, IWSA Workshop, Paris, 1993.

(30) Legube, B., M. Bourbigot, A. Bruchet, A. Deguin, A. Montiel, and L. Matia, "Bromide/Bromate Survey on Different European Water Utilities", Proceedings, International IWSA Workshop, Paris, 1993a.

(31) Neta, P., R. Huie, A. Ross, J.Phys. Chem. Ref. Data, 17:3, 1988

(32) Ozekin, K. , M. Siddiqui, G. Amy, W. Haag, "Pathways For Bromate Formation in NOM-Free Water", AWWA Annual Conference, New York, 1994.

(33) Richardson, L., D. T. Burton, and G. R. Helz, "Residual Oxidant Decay and Bromate Formation in Chlorinated and Ozonated Sea-Water", Water Research, 15:1067. 1981.

(34) Siddiqui, M., "Factors Affecting DBP Formation During Ozone-Bromide Reactions", Ph.D. Dissertation, University of Arizona, 1992.

(35) Siddiqui, M. and Gary Amy, "Factors Affecting DBP Formation During Ozone-Bromide Reactions" Journal. AWWA, 85:1, 1993.

(36) Siddiqui, M., G. Amy, K. Ozekin, K. Miller, and P. Westerhoff, "The Role of Relating Pilot-Scale Tracer Data with Bench-scale Data For Bromate Prediction", 11th Ozone World Congress, San Francisco, CA, 1993a.

(37) Siddiqui, M. and G. Amy, "Empirical and Analytical Models For Ozone DBPs Prediction", Ozone: Science & Engineering, 16(2), 1994.

(38) Siddiqui, M, G. Amy, K. Ozekin, W. Zhai, and P. Westerhoff, "Alternative Strategies for Bromate Removal from Drinking Water", Submitted to JAWWA for Publication, 1994a.

(39) Siddiqui, M., G. Amy, K. Ozekin, "Bromate Formation During Ozonation: Effect of NH_3/Br ratio", 12th Ozone World Congress, Lillee, France, 1995.

(40) U.S. Environmental Protection Agency. "Monitoring Requirements for Public Drinking Water Supplies; Proposed Rule", Federal Register, 59(28):6331-6444, 1994.

(41) von Gunten, U., J. Hoigne, A. Bruchet, "Bromate Formation During Ozonation of Bromide Containing Waters", 51-56, IWSA Workshop, Paris, 1993.

(42) von Gunten, U., and J. Hoigne, "Factors Affecting the Formation of BrO_3^- During Ozonation of Bromide-Containing Waters", *J. Water SRT-Aqua* 41:5, 1992.

(43) Wajon, J.E. and Morris, "Rates of Formation of N-Bromoamines in aqueous Solution", J. Inorganic Chemistry, 21:4258-4263, 1982.

(44) Westerhoff, P, G. Amy, R. Minear, M. Siddiqui, R. Song, and K. Ozekin, "Bromate Formation in Laboratory Studies: Influence of Water Quality and Treatment Variables", 1993 AWWA Annual Conference, San Antonio, Texas, 1993.

(45) Yates, R.S., and Stenstrom, M.K., "Bromate Production In Ozone Contactors", AWWA Annual Proceedings-San Antonio, 1993.

(46) Yamada, H., "By-Products of Ozonation of Low Bromide Waters and Reduction of the By-Products By Activated Carbon", ppS-9-58, Proceedings, 11th Ozone World Congress, San Francisco, 1993.

(47) Xiong, F., J. Croue, and B. Legube, "Long-Term Ozone Consumption By Aquatic Fulvic Acids Acting As Precursors of Radical Chain Reactions", Environ. Sci. Technol, 26:1059-1064, 1992.